Irradiation Effects to Insulators and Their Application to UWCTR

P.A. Sanger

March 23, 1973

UWFDM-59

FUSION TECHNOLOGY INSTITUTE

UNIVERSITY OF WISCONSIN

MADISON WISCONSIN

Irradiation Effects to Insulators and Their Application to UWCTR

P.A. Sanger

Fusion Technology Institute
University of Wisconsin
1500 Engineering Drive
Madison, WI 53706

http://fti.neep.wisc.edu

March 23, 1973

UWFDM-59

Irradiation Effects to Insulators and Their Application to UWCTR

by

Phillip A. Sanger

March 23, 1973

FDM 59

I. Introduction

The use of insulating materials in radiation environments has been studied extensively in the past due to the advent of space exploration and nuclear reactors. The complexity of the problem was enormous. Each polymer, with its unique bonding and structure, had to be treated separately. Even though several basic damage mechanisms can be postulated, the predominance of no one mechanism can be predicted with any certainty apriori. The approach adopted then was to simply irradiate a variety of polymers and measure their properties as a function of dosage. Needless to say, this led to a multitude of irradiations at a variety of conditions and was a herculean task. The aim of the present paper is to evaluate the radiation-induced property changes to be expected in the insulating materials used in UWCTR. The conclusions will be obtained from the aforementioned experimental data.

In UWCTR insulating materials are found both in the magnet system and in the blanket. Four different locations can be specified (see figures 1 and 2) and the role that the insulator plays at each location will be described.

Location 1 (figure 1): The cryogenic system makes use of a thermal insulation known as superinsulation. In order to reduce the amount of refrigeration required to keep the superconducting magnet at $4.2^{\circ}K$, it is necessary to thermally isolate the magnet from the exterior at $300^{\circ}K$. Heat transfer by conduction is stopped by introducing a vacuum space between the two temperatures. However radiative

heat transfer, which varies as

$$e\sigma(T_1^4 - T_2^4)$$

where σ = the Stefan-Boltzmann constant
e = emissivity
T_1, T_2 = the surface temperatures

must also be reduced. This can be done using material with a high reflectivity and a low effective thermal conductivity. Superinsulation, a composite of polyethylene terephthalate (trade names of Mylar, Dacron, or Terylene) and aluminum, is such a material. A thin layer of aluminum (300^{o}A) is vapor deposited on a sheet of Mylar(6.3 microns). A low thermal conductance is achieved by crinkling this insulation thereby allowing only point contact between successive layers. Thermal isolation is therefore attained through a combination of vacuum and many layers of superinsulation (typically 100 layers/inch). It is essential that the mechanical integrity of the insulation after extended periods of irradiation be guaranteed such that no line of sight to the 4.2^{o}K surface exists.

Location 2 (figure 1): The magnet system also needs electrical insulators within the windings themselves to prevent the development of electrical short circuits. A short circuit in the magnet has several undesirable effects: a) sudden changes in inductance and field distributions, b) delayed current charging times and c) increased risk that a localized short circuit will absorb the magnet energy in the case of a quench. The interlayer electrical insulation in UWCTR will be a glass fiber reinforced, mineral filled, aromatically cured epozy. Several types are available but

either Epon 828 or Bond Master E645 will be used. In addition to acting as an insulator, this epoxy will serve as the bond between the stainless steel reinforcing and the conductor itself. The insulator will experience the maximum stress both at room temperature in the prestressed condition and the 4.2°K under magnetic loading. At those times, a bond strength of 50 to 100 psi and a compressive strength of 1000 to 2000 psi will be demanded from the epoxy composite. The tensile stress in the epoxy will probably be negligible.

Location 3 (figure 1): In the final assembly of the magnet system, use is made of an insulating spacer between each successive disc to allow contact of the coolant with the conductor edge. The stresses that will be applied to this spacer come from the magnetic field gradients. The effectiveness of this spacer then depends on its compressive strength during irradiation. The material proposed for this spacer is referred to by its tradename of Micarta. Micarta consists of linen fabric soaked in epoxy which is then hardened. The determination of its properties under irradiation will be one aim of this paper.

The use of high magnetic fields imposes severe demands on the bond strength and the compressive strength of the epoxy-fiber glass composites, on the compressive strength of Micarta, on the dielectric strength of the epoxy-fiber glass composite and on the mechanical integrity of the superinsulation.

Location 4 (figure 2) The blanket also has need of insulators which are somewhat different than in the magnet system.

A Tokamak reactor can be viewed as a large transformer with the plasma serving as the secondary. In order for the electric field to penetrate to the plasma and induce a current, at least one nonconducting gap must be left in the blanket. If no gap in the highly conducting blanket is provided, the primary of the transformer will not be able to induce sufficient current in the plasma to continue the operation of the reactor. It may not be necessary to extend the insulator completely to the first wall since the operating densities of the fuel mixture, in terms of pressure, are very low (a few microns of mercury). In terms of dielectric strength, this low pressure might be adequate to fulfill our needs. A possible arrangement is shown in figure 2. The insulator, which could serve as the vacuum seal, may be placed as far from the first wall as necessary to minimize radiation damage. One aim of this paper then is to determine how far into the blanket region this insulator must be placed to attain a reasonable lifetime for this component. It will be seen later that an inorganic insulator such as Al_2O_3 or MgO would be a preferred choice. In contrast to insulators in the magnet system, these insulators will operate at high temperatures (550°C or more).

II. Irradiation Effects to Insulators

Irradiation effects to metals have been treated in an earlier paper.[19] The primary damage mechanism to metals is the displacement of the metallic atom from its equilibrium site in the crystalline matrix. This damage mechanism is also predominant in inorganic materials which possess a crystalline

structure. When considering only displacements in these materials, we have neglected the primary method of energy loss of energetic particles, that of electronic excitation and ionization. As much as 90% of the energy of PKA's can be dissipated in this manner. This method of energy loss can be ignored as a damage mechanism in metals where the electrons are loosely bound and are relatively free to move within the structure. However this is not the case for organic and inorganic materials where ionic and covalent bonds are important. The excitation and ionization of electrons in organic materials causes permanent chemical changes within the solid as well as a temporary photo-conductivity. Inorganic materials also exhibit temporary photoconductivity but are permanently damaged by displacements due to their crystalline structure. The addition of the electronic component of the energy loss is more critical when one realizes that the composition of polymers is predominantly low Z materials. The average amount of energy transferred to light atoms is greater than for heavy atoms and the percentage of that energy which is lost as electronic excitation and ionization is also higher.

The importance of electronic excitation and ionization dictates that sources of radiation, which could be neglected when only displacements were considered, now must be included. The most important of these sources is the photon or gamma flux, which interacts with the electrons of the solid through the photoelectric effect, compton scattering and pair pro-

duction. For most polymeric materials, the photoelectric effect can be neglected. The energetic electrons which result from the remaining two interactions, however, cause very few displacements but very large electronic perturbations.

A. Polymers

Polymers are primarily organic materials consisting of carbon, hydrogen, oxygen, and perhaps nitrogen bound together in various ways. These molecules derive their name from the fact that they are made up of many identical smaller units or "mers". These mers are linked together by covalent bonds and, in the case of linear polymers, form long chains. Each separate chain is linked to its neighbor by chain entanglements or by hydrogen bonds. The repeating units of several different polymers are shown in figure 3 including the common polymer, polyethylene, and the more complicated polymer, polyethylene terephthalate. Notice the benzene ring in mylar. This configuration is very stable and has a good effect on the radiation resistance of this material.

As was mentioned previously, the atoms of a polymer are bound together by covalent bonds. Such covalent bonds can be ruptured by the addition of radiation energy. Organics differ in this respect from ceramics and metals in that the latter are primarily crystalline and generally do not contain covalent bonds. Radiation can induce structural changes in polymers where covalent bonds are broken and new

bonds formed. An important characteristic of radiation damage to polymers is its irreversibility which is a direct consequence of the reconstruction of these broken bonds into a different structure.

Chemical changes due to radiation are generally reported in terms of a yield or G-value. The G-value of a reaction is defined as the number of changes per 100 eV of energy absorbed by the material. The G-value for crosslinks is then the number of polymer chains crosslinked per 100 eV.

The major chemical changes that will be considered in the following sections are a) crosslinking, b) chain fracture, c) oxidative degradation, d) gas evolution and e) color changes. These radiation-induced changes have been treated in detail by Charlesby[1] and only a brief summary will be presented here.

1. Crosslinking

The term crosslink refers to a junction point or tetrafunctional link between two polymeric chains. In a study of radiation effects, it is assumed that the crosslinks are produced at random along the molecular chains.

This assumption is not completely true since it is known that the various bonds are not of equal strength, that is, C=C is stronger than H-H which is stronger than C-H which is stronger than C-C which is stronger than C-N etc. It is reasonable to assume that the weaker bonds of a polymer would be more susceptible to radiation damage. Therefore within a monomer unit, certain bonds will be preferentially damaged. Nevertheless the assumption of randomness would be close to valid for long polymers of many monomer units, the randomness being defined with respect to the monomer as opposed to the bond.

When a crosslinking polymer is irradiated, the links formed between chains decrease the number of separate molecules. At some radiation dosage, the crosslinks are so numerous that the molecules for a closed, three dimensional network or gel. The point at which an insoluble network first begins to form is termed the gel point and the corresponding radiation dose is the gelling dose. This condition is reached when δ, the average number of crosslinked units per weight average molecule, is equal to 1.

Most physical properties show dramatic changes for doses equal to or greater than the gelling dose. One of the most significant property change is the effect on swelling. For $\delta < 1$, a solvent such as benzene or water can dissolve the polymers. The three dimensional network, which forms for $\delta > 1$, traps the solvent atoms much like a net catches fish. Highly crosslinked polymers ($\delta >> 1$) have become too rigid to accept the solvent and therefore the swelling decreases.

Figure 4 illustrates this sequence.[1] This susceptibility to absorption of solvents such as water can result in a dramatic drop in dielectric strength and damage to an insulation.

2. Degradation

The effect of radiation on certain polymers results in longer chains through crosslinking. Other polymers experience a breaking up of the chains due to radiation. Many polymers show both effects simultaneously. A general rule of thumb with many exceptions can be used to determine which mechanism will predominate: Monomer units with two side chains will fracture or degrade while those with single or no side chains will crosslink. Hydrogen is not considered to be a side chain in this criterion.

Degradation is the term given to the scission of main chain bonds by radiation. The result of degradation is a decrease in molecular weight and the formation of chain fragments usually different than the monomer unit. The precise mechanisms are still very much in doubt but all processes involve some kind of radical formation.

All polymers experience degradation at the end of life. Once a polymer has been highly crosslinked the only mechanism available would be degradation. Those polymers exhibiting degradation as the principal form of radiation damage can be considered to be more sensitive to radiation. The result of degradation is an extreme crush sensitivity and the tendency to powder.

3. Oxidative Degradation

Due to the high electron affinity of oxygen and to its reactions with free radicals, the presence of oxygen can readily modify radiation damage mechanisms. The effect of oxygen can easily be detected in some materials by the presence of CO_2 and H_2O and by a net increase of weight. The reaction of oxygen with free radicals reduces the number of radicals available for crosslinking (see figure 5). The degree to which these reactions affect the physical properties of the materials is probably dependant on the diffusion rate of oxygen in the matrix and on the geometry of the specimen, e.g. thickness.

4. Gas Evolution

The evolution of gas from irradiated polymers was one of the first radiation effects to be detected. The general effect of radiation is the production of radicals which occurs predominantly at the expense of the C-H bond. Once the radical has reacted in a manner other than recombination with the hydrogen ion, such as crosslinking or unsaturation (the formation of a carbon double bond), the hydrogen is free and soon forms a hydrogen molecule with another free hydrogen atom. The free hydrogen atom may also force unsaturation by stripping a hydrogen atom from the polymer. Eventually these molecules diffuse to the surface and are released. The overall effect is to decrease the hydrogen to carbon ratio, drastically affecting the physical properties of the material. This effect is shown in figure 6 for polyethylene.

5. Coloration

In addition to the above changes, many materials change color due to the liberation of electrons, which become trapped at positive ion vacancy sites to give F-centers. Characteristic absorption bands are produced which can be bleached out either optically or thermally. The trapping site may also be an impurity center, or possibly a strained part of the structure. These sites may then interact with radiation induced damage resulting in a shifting of the absorption bands with increasing fluences.

6. Effect of Temperature

It can certainly be said that there definitely is a temperature dependance for damage mechanisms. The source of this dependance is still under debate. Figure 7 shows the influence of temperature on several different G-values:$G(H_2)$, G(crosslinks) and G(unsaturation). Both the irradiation and the measurements were performed at the temperature indicated. At low temperatures, the simple relation, $G(H_2)$ = G(crosslinks) + G(unsaturation), is approximately true. All G-values tend to increase with temperature corresponding to an activation of about .004 eV for $T < -100^{\circ}C$. At higher temperatures, G(crosslinks) increases rapidly with an activation energy ten times higher resulting in a five fold increase of G. The other G-values show little variation. This rapid increase of G(crosslinks) is thought to be due end effects and side chain fracture since simple crosslinking due to hydrogen abstraction is not indicated, i.e. $G(H_2)$ remains approximately constant.

7. Radiation Protection

The history of radiation damage to polymers is such that the major emphasis has been on making polymers serviceable in a radiation environment. Most of the methods that improve the radiation stability of polymers have been found through a trial and error approach. The answer to the question "Why does some method work?" has been largely neglected. It is now appropriate to point out some of the methods.[2]

a) Mineral fillers such as ground glass and Al_2O_3 increase the radiation stability of polymers through a mechanism that is poorly known.

b) For polymers that must operate in the presence of oxygen, oxidizing agents can be introduced to act as oxygen scavengers.

c) Aromatic ring systems may act as "energy sponges". These structures are strong enough to withstand a high energy content until the energy can be dissipated as heat.

d) Radiation attacks the weakest bonds first. Therefore, by adding weak bonds located in noncritical places, the system is provided with sacrificial bonds reducing the damaging radiation effects.

8. Specific Materials

Several review articles have been published that give a comprehensive survey of irradiation effects to polymers.[1-6] Selected graphs and tables are shown in figures 8-10. The start of the moderate to severe range of damage in figure 8 is equivalent to the 25% damage level defined in the other

figures. The damage that is observed has always been a degradation of one or more of the mechanical properties of the polymer, e.g. ductility, compressive strength. Bopp and Sisman[5] have also attempted to list different monomer units with respect to radiation stability (figure 11). Most of the studies were done in the 1950's and are difficult to obtain. One is led to assume that the irradiations were at room temperature and in air but, without the original data, one cannot be certain. In the listing of radiation stability, the beneficial effect of the benzene rings are clearly seen, with the one notable exception of mylar. The present author takes exception with Bopp and Sisman on this point and would place mylar high on the scale of stability equal to or better than polyethylene. The experimental data clearly supports this position change. Certain materials will be treated in more detail in the following sections.

a) Polyethylene

Damage Threshold: 19 Megarads (abbrev. Mrads.)

25% Damage Level: 93 Mrads

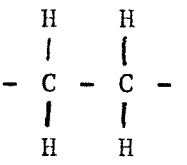

This polymer is typical of those that crosslink under radiation. Hydrogen gas is evolved, the unsaturation is increased, and the small regions of crystallinity, originally present, are destroyed. Polyethylene is extremely sensitive to the presence of oxygen during irradiation. Like most polymers, it acquires a yellow tinge during irradiation. This polymer can be characterized by a glass-like structure

at high radiation deses and becomes extremely brittle.

b) Polytetrafluorethylene (Teflon)

Damage Threshold: 1.7 x 10^{-2}Mrads

25% Damage Level: 3.7 c 10^{-2}Mrads

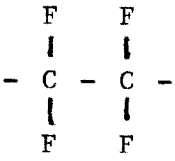

Teflon has been found to have a low radiation resistance. The primary damage mechanism is main chain fracture or degradation. At low loses (3.4 x 10^{-2}Mrads), this polymer becomes sticky, turning to an extremely brittle material by 1 Mrads. The sensitivity of Teflon to radiation can be partly explained by the difference in bond energies of C-H and C-F, the former going to a H_2 molecule in an exothermic reaction while the formation of a fluorine molecule is a highly endothermic reaction.[1] It is believed that the liberated fluorine atom does not form a molecule

$$H + -CH_2- \quad H_2 + -\dot{C}H- + 13 \text{ Kcal/mole}$$

$$F + -CF_2- \quad F_2 + -\dot{C}F- - 68 \text{ Kcal/mole}$$

but instead interacts with its own radical to cause a main chain scission at the C-C bond. This possibility is given further credibility by the fact that the C-C bond in Teflon is stretched due to the large size of the fluorine atoms. The C-C bond is thus more susceptible to scission.

c) Polyethylene Terephthalate (Mylar)

Damage Threshold: 30 Mrads

25% Damage Level: 120 Mrads

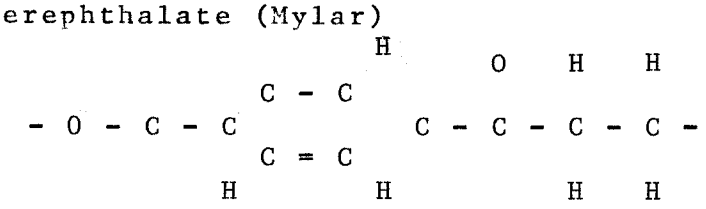

This polymer can be expected to possess good radiation resistance due to the presence of the benzene ring and the

ethylene structure. The predominant damage mechanism is crosslinking. In the highly drawn fiber state, this polymer will undergo degradation, rather than crosslinking. Figure 10b shows the effect of oxygen on the radiation resistance.[4] Vacuum irradiations of mylar resulted in decreases in elongation and in tensile strength of -23%. Similar irradiations in air resulted in 30% and 34% decreases respectively. In the absence of oxygen during irradiation, a number of -COOH- end groups are formed whereas, in the presence of air, the group -OH and C=O are obtained.[1]

Several measurements have been made on the electrical properties of mylar. Figure 12 shows that the damage threshold for the electric strength of mylar appears at approximately 100 Mrads of electron radiation and degrades to 25% of its preirradiation value by 200 Mrads, and to 50% by 1000 Mrads.[7] The volume resistivity of mylar has been measured using 14 MeV neutrons as the source of radiation.[8] A decrease of 33% in the static volume resistivity was reported for a total fluence of 10^{11} n/cm^2.

d) Phenol Formaldehyde with linen fabric filler (Micarta)

Damage Threshold: 0.34 Mrads

25% Damage Level: 3.2 Mrads

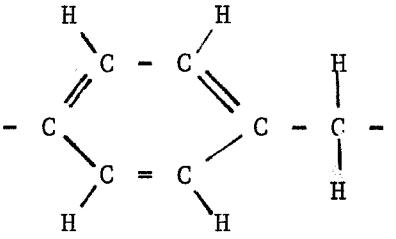

The principal reason for the radiation sensitivity of micarta is the decomposition of the filler. The binder, phenol formaldehyde, has a threshold of 2.7 Mrads and the use of paper or linen as the filler has only a detrimental effect. Micarta swells, becomes brittle and loses all of

its tensile and impact strength at 100 Mrads. The swelling and gas evolution is primarily due to the filler. The use of asbestos as filler in fabric, fiber or powder form drastically improves the radiation resistance of this composite. The resulting radiation stability improves as one moves from fabric to fiber to powder.

e) Epoxies (Example of mineral filled glass fiber reinforced DER 332 as a typical case)

Damage Threshold: 8000 Mrads 25% Damage Level: 50,000 Mrads

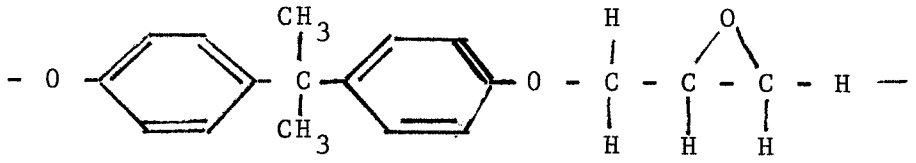

The epoxies that will be considered here, have three major components: 1) organic binder (structure shown in diagram), 2) mineral filler normally Al_2O_3 (900 mesh) and 3) glass fiber reinforcing. Common mechanical properties for epoxies of this type are shown in figure 13. Radiation effects are tabulated in figure 14. These values are the result of experiments carried out by Brechna.[9] Figures 15,16 and 17 show the relative change in bond strength, compressive strength, and impact strength for DER 332. The impact strength is the first property to be affected reaching its threshold at about 300 Mrads. Bond and compressive strength reach threshold by 10^4 Mrads. The electrical properties have also been studied in the same experiments. Figures 18 and 19 show the effect of radiation on the insulation resistance and the dielectric strength of this composite insulation. The volume resistivity shows an order of magnitude

decrease at a dose of 10^4 Mrads but this is not considered to be of great practical significance since the resistivity is still approximately 10^{14} ohm-cm. The dielectric strength of dry DER 332 samples was not affected by irradiation but Epon 828 samples showed a 20% decrease after a dose of 1.2×10^6 Mrads. However the significant effect that was brought to light in these irradiations was the severe degradation of dielectric strength due to the enhanced moisture absorption capabilities of the epoxies. Figure 20 shows that, after a dose of 10^6 Mrads, a saturation of moisture content occurs after three days of immersion. The dielectric strength degradation saturates out after only 30 hours of immersion and lowers the corona threshold by 80%.

B. Ceramic Materials

Ceramic materials are, in general, more resistant to radiation damage than are the organic polymeric materials. It has already been pointed out that most of the energy of a neutron is deposited in polymers as electronic excitation. A polymeric solid is held together by covalent bonds and therefore perturbation of the electron structure has large permanent effects. Ceramics and metals, on the other hand, have a crystalline structure and the electronic excitation has little effect on the atomic ordering. Displacements are, then, the predominant source of permanent radiation damage to ceramics whereas they constitute only a small part of the damage in polymers. In addition electrons and gamma radiation have little or no effect on the radiation damage. It should be pointed out however that the energy lost by

ionization and excitation induces a photoconductivity both in ceramics and in polymers alike. Of course, in metals, no photoconductivity is measured since there are many electrons already in the conduction band and the radiation induced component is negligibly small. This phenomena will be discussed in more detail in a later section.

Figure 21 illustrates the relative radiation resistance of the important ceramic materials for use in a radiation environment.[3] Note that these rankings are based on changes in physical properties induced by neutron damage. In the following paragraphs, the three major ceramics, Al_2O_3, MgO and BeO, will be treated in detail with respect to lattice expansion, density, thermal conductivity, electrical resistance, and mechanical properties.

1) Alumina (Al_2O_3) A comprehensive tabulation of the radiation studies completed on Al_2O_3 prior to 1964 is shown in figures 22 and 23[2]. Few studies have been made since that time, although more study is warranted due to the importance of this insulator in fusion reactors, especially those using the theta pinch concept. This ceramic exhibits anisotropic expansion similar to graphite but on a smaller scale. Figure 24 demonstrates that expansion is greater parallel to the c-axis than perpendicular to the c-axis. However this expansion is small reaching .05% at 10^{19} n/cm^2 (E > thermal). The density changes are more significant and reach an increase of 6.8% for a sintered polycrystalline Al_2O_3 after 4×10^{20} n/cm^2 (E > 100eV).[11] Single crystals showed a small decrease in density, 1% after

approximately the same fluence. All of these irradiations were done at 50°C.

The thermal conductivity of Al_2O_3 was reduced by 78% after 4×10^{20} n/cm^2(E > 100eV) at 50°C.[12] Changes in electrical resistivity have been reported after 3.5×10^{18} n/cm^2 at 400°C.[13] A two order of magnitude decrease in resistivity was found and attributed to the trapping of electrons in vacancy sites.

The mechanical properties of Al_2O_3 seem to be less affected by irradiation. Young's modulus decreased 10% after exposure to 1.6×10^{20} n/cm^2 at 50°C.[12] While no reports were available on strength characteristics, it would seem probable that the polycrystalline material might experience severe internal stresses due to the anisotropic swelling.

2) Magnesia (MgO) Figure 25 presents a summary of the work completed on this ceramic.[2] It is evident that little work has been done compared to the numerous works on Al_2O_3. Less than 1% changes in density were reported for MgO after fluences of greater than 10^{21} n/cm^2 (E> thermal).[2] The thermal conductivity showed a 40% decrease after 3×10^{19} n/cm^2(E 100eV) at 50°C. Changes in electrical resistivity were essentially the same as that of alumina.

Relatively little work has been done on this ceramic that no definite predictions can be made. There is the possibility that MgO might be more dimensionally stable than Al_2O_3 or BeO. This prediction is based on the knowledge that MgO has a much simpler crystalline structure (NaCl) than do the latter two ceramics.[2] Little experimental work in

this regard has been performed to either prove or disprove this hypothesis.

3) Beryllia (BeO). The effects of radiation on BeO has been the most studied of all ceramics, excluding perhaps the fuel oxides, UO_2 and PuO_2. BeO can be used as a moderator in thermal reactors and was considered as good material for fuel dispersion systems.

The fractional growth and lattice parameter change for a variety of BeO samples are shown in figures 26 and 27.[14] At high fluences it is believed that the formation of helium and tritium gas bubbles continues the growth instead of saturating as the lattice parameter changes would indicate. Calculations by Clarke[14] indicated that as much as 70 ppm of He and 2 ppm of tritium can be produced after a fluence of $10^{21} n/cm^2$ ($E > 1$ MeV, reactor spectrum). Figure 28 shows that, at high temperature, the tritium will diffuse out of the sample whereas hydrogen, at low temperatures, and helium, at all temperatures, will stay in the sample and cause swelling.[15]

Since BeO has not been proposed as an insulator, its electrical properties have not been investigated. On the other hand its mechanical properties have received extensive treatment.[16] Figure 29 indicates severe degradation of the crushing strength (only 25% of original) at a fluence of $6 \times 10^{19} n/cm^2$ ($E > 1$ MeV) at an irradiation temperature of $100^{\circ}C$. However, for a temperature of $350^{\circ}C$, BeO shows only a 50% decrease at a fluence of $2 \times 10^{20} n/cm^2$.

An overall summary of these three ceramics seems to indicate that swelling (anisotropic for Al_2O_3 and BeO) accompanied by a reduction of electrical and thermal conductivity will result from neutron radiation. High initial densities are more radiation stable and high irradiation temperatures result in a much smaller degradation in mechanical properties.

C. Radiation Induced Photoconductivity

A large part of the energy of incident radiation is absorbed through electronic excitation and ionization. A higher mobility of charge carriers in the insulator and excitation-produced quasi-free electrons are the result of this energy deposition. Harrison et. al.[17] have investigated this phenomena in detail and divide it into three regions (Figure 30). In region A the conductivity rises exponentially after the commencement of radiation. This rise is characterized by

$$(\sigma-\sigma_o) = A \quad (1-e^{-t/\tau_o})$$

where

σ = initial conductivity

σ = conductivity at time t

A = empirical constant

$\tau_o = k_o \dot{\gamma}^{-\mu}$ = time constant of the response as a function of gamma dose, gamma equivalent ionizing dose, or dose rate k_o and μ being empirical constants

In region B the conductivity has found its equilibrium value and its magnitude is a function of dose rate and the temperature. The equilibrium value can be derived from the empirical relation

$$(\sigma-\sigma_o) = A_\gamma \dot{\gamma}^{\sigma}$$

where

A_γ and σ = empirical constants (see Table 1) and

$\dot{\gamma}$ = gamma or gamma equivalent (ionizing) exposure rate in rads $(H_2O)/s$.

This induced conductivity then decays to near its initial value after the cessation of irradiation with a certain time constant. Figures 31 and 32 gives some experimentally determined values for the previously presented relation for selected polymers. For inorganic materials δ is almost always 1 and A_γ is approximately 10^{-16} to 10^{-18}. An interesting experiment has been performed using .5 Kev hydrogen ions.[18] At an ion current of 300 microamps, the conductivity of Al_2O_3 and MgO was seen to increase by more than 5 orders of magnitude without reaching its saturation value. The importance of this report can be realized if one considers the possibility of deuterium and tritium ions with energies of 10 KeV or more impacting on the insulating material of a fusion reactor, particularly a theta pinch reactor.

Since this induced conductivity is due to the liberation of electrons, this effect would be expected to occur by simply raising the temperature. The work of Dau and Davis[23] indicates that the photoconductivity is masked out by the thermally-induced conductivity at temperatures as low as 300°C in MgO and Al_2O_3. For a fusion reactor, the thermally induced component will then dominant and the photoconductivity can be neglected.

III. Application to UWCTR

The aim of this paper is to establish the radiation dose limits to which the insulating components of UWCTR can be taken and still remain serviceable. A judgment must be made as to what degradation in properties is deemed acceptable. In previous sections an attempt has been made to acquaint the reader with the demands made on the polymers in UWCTR. A brief review of those demands and the radiation damage limits that they impose are discussed in the following sections.

The cryogenic system demands simply that the superinsulation occupy the vacuum space between room temperature and liquid helium temperature and that no line of sight exists between the two temperatures. A criterion for the superinsulation damage limit has then been established taking into account the passive role of this material. Let D(material) represent the limiting dose for the material in question. D(mylar) then corresponds to a 90% reduction in initial elongation (35% reduction in tensile strength) and is equal to 550 Mrads(figure 33). The remaining 10% initial elongation is kept as a safety factor and to safeguard against shocks and vibration that may occur in the UWCTR system. A completely optimistic criterion would be defined at much less than 10% initial elongation and less than 5% initial tensile strength and allows a total dosage of 2000 Mrads. A material in such a condition would simply crumble at the slightest disturbance.

The interwinding epoxy insulation must have a bond strength

of 100 psi, a tensile strength of 4500 psi, a compressive strength of 2000 psi and a dielectric strength of approximately 1 kV. The data given in figure 19 for the dielectric breakdown strength shows that this property is relatively insensitive to radiation at doses where the mechanical properties are seriously degraded. The validity of this statement depends on the amount of humidity present in the material but the author assumes that proper precautions have been taken during construction and warm-up periods to insure minimal water condensation within the dewar. The radiation damage to the epoxy is then only a function of its mechanical properties. The strengths listed above correspond to 4%, 8% and 4% respectively for the initial values of bonding, tensile and compressive strength of Epon 828/1031. D(epoxy) for these limits are shown in Table 1.

Table 1

Dose limits and criterions used in their establishment for the insulating components of UWCTR (based on data at room temperature)

Material	Radiation Limit (Megarads)	Criterion (per cent of initial property remaining)
Mylar a)	550	10% elongation 65% tensile strength
b)	2000	<<10% elongation <5% tensile strength
Epoxy (Epon 828/1031 mineral filled glass fiber reinforced)	10^6 10^6 3×10^5	4% compressive 4% bonding 8% tensile

Phenolic		
linen fabric	2.3	10,000 psi
asbestos fiber	300	10,000 psi
glass cloth	7.4×10^4	~10,000 psi.

The mechanical stresses on the phenolic spacers have as yet not been calculated. An approximation can be arrived at though using the NAL Bubble Chamber Magnet as a benchmark and scaling the stresses as the square of the magnetic field. Assuming a 75% coverage of the spacers between each successive disc, the spacers will be submitted to a compressive stress of 10,000 psi. The author suggests the use of either asbestos fiber phenolic (compressive strength of 12,200 psi.) or glass cloth phenolic (compressive strength of 60,000 psi.). For the asbestos fiber phenolic, the 18% allowed degradation corresponds to 300 Mrads. Radiation damage to the glass cloth phenolic is not available but could be expected to behave similar to the glass fiber laminated epoxy of figure 14 reaching damage threshold at 2500 Mrads and a tensile strength of 10,000 psi at 7.4×10^4 Mrads.

The detailed application of inorganic radiation damage will be presented in a supplement to the present paper due to the discovery of new data and to the vagueness of the service requirements demanded by UWCTR.

The author feels that, at this time, several points must be made in order to place the preceding limits in perspective. All of the above limits have been based on data obtained at room temperature and above. From figure 7 and the data of

Mowers[22], the conclusion can be drawn that cryogenic irradiation might result in less damage at a given dose and quite possibly change the property which is first affected. No irradiations have been carried out at 4.2°K even though a few works have dealt with damage at liquid hydrogen temperatures (20°K).[22]

Beneficial effects will also be seen at low temperatures simply because the absolute strengths are improved. Increases of 70% in strength are easily obtainable between 300°K and 20°K for glass cloth reinforced materials. The increases are much less for the other phenolic composite materials but are still substantial.[22]

IV. Conclusions

The conclusion that can be drawn from Table 1 are stated as follows:

1) The mineral filled, glass fiber reinforced epoxy is highly radiation resistance and retains its design properties to very high doses.
2) The linen fabric phenolic spacers are extremely sensitive to radiation and would limit the UWCTR to a low dosage. By the suitable choice of asbesto fiber phenolic or glass cloth phenolic, the dose limit could be raised substantially (see Table 1).
3) The deterioration of mylar under irradiation appears to limit the design of the UWCTR magnet shield. The properties have been allowed to degrade to the lowest limit designable. Thus the magnet shield shield must allow a dose of approximately 550

Mrads to the superinsulation.

Figure 36 represents, in bar graph form, the various limiting radiation doses for the insulating magnet components. In the same figure the limits for the metallic components are shown in terms of dpa.[19] Two cautions should be given to the reader on the use of these graphs. The realization of the significance of the rad unit is of primary importance. This unit is defined as 100 ergs of energy deposited per gram of the specific material in question. Consider now a 1 MeV neutron incident on a predominantly hydrogenous material. The energy deposited by the neutron in this case is considerably more than the energy deposited by the same neutron in a predominantly carbonic material. From figures 33, 34 and 35 the reader can see that the difference can be as much as a factor of 3.

The second word of caution is directed to the dpa values. The dpa unit is a strong function displacement energy which varies significantly from metal to metal. Again the correlation from one material to another is not one to one with respect to neutron fluence. The final comment is to point out that the relation between rads and dpa is complex and a strong function of the neutron energy spectrum.

As in the case of the metallic components, two areas present themselves as candidates for further investigation. These areas can be defined as follows:

1) the radiation behavior of the composite of mylar and aluminum in the temperature range 300-4.2^{o}K,

2) the radiation damage of polymers and polymeric composites at liquid helium temperatures.

With the additional information that these studies would provide the radiation damage to insulating components would be complete.

References

1. A. Charlesby, Atomic Radiation and Polymers, (Pergamon Press, New York), 1960.

2. J.F. Kircher and R.E. Bowman, Effects of Radiation on Materials and Components, (Reinhold Publishing Co., New York), 1964.

3. C.L. Hanks and D.J. Hamman, Radiation Effects Design Handbook, Section 3: Electrical Insulation Materials and Capacitors, NASA-CR-1787 (1971).

4. R. Harrington and R. Giberson, "Chemical and Physical Changes in Gamma-Irradiated Plastics", Modern Plastics, 36, 199 (1958).

5. O. Sisman and C.D. Bopp, "A Summary of the Effect of Irradiation on Some Plastics and Elastomers", ASTM Spec. Pub. 208, 119 (1956).

6. N.J. Broadway, Radiation Effects Design Handbook, Section 2: Thermal Control Coatings, NASA-CR-178 6 (1971).

7. E.L. Brancato and J.G. Allard, "Effects of Electron Irradiation on Electrical Properties of Mylar," AIEE Summer Meeting (Montreal, Canada), June 24-28, 1957.

8. A.P. Bazin, "Effect of the Bremsstrahlung Radiation from a 25 MeV Betatron and of 14 MeV Neutrons on the Electrical Conductivity of Polymeric Dielectrics," Soviet Phys.-Solid State, 4 (10), 2113 (1963).

9. H. Brechna, "Effect of Nuclear Radiation on Organic Materials; Specifically Magnet Insulation in High Energy Accelerators," SLAC Rep. No. 40, AEC Contract AT(04-3)-515 (1965).

10. K. Little, "Effect of Irradiation on Nylon and Polyethylene Terephthalate," Nature, 173, 680(1954).

11. J.J. Antal and A.N. Goland, "Study of Reactor Irradiated α - Alumina," Phy. Rev., 112, 103(1958).

12. J.H. Crawford and M.C. Wittels, "Radiation Stability of Nonmetal and Ceramics," Second United Nations International Conf. on Peaceful Uses of Atomic Energy (Geneva, Switzerland), 5,300(1958).

13. G.W. Monk, "Refractory Dielectrics in a Reactor", WADC-TR-57-599 (1957).

14. F.J.P. Clarke, "Irradiation Damage in BeO," AERE-R-3971 (1962).

15. R.P. Shield, J.E Lee and W.E. Browning, "Effect of Fast Neutron Irradiation and High Temperature on BeO," ORNL 3164 (1964).

16. J. Elston and C. Labbe, "Effect of Heat Treatment and Neutron Irradiation on Physical and Mechanical Properties of BeO Sintered Under Load," J. Nucl. Mat., 4, 143 (1961).

17. S.E. Harrison, F.N. Coppage and A.W. Synder, "Gamma Ray and Neutron Induced Conductivity in Insulating Material," IEEE Trans. Nuc. Sci., 10 (5), 159 (1963).

18. L.B. Griffiths, "Effect of Hydrogen Ion Bombardment on Al_2O_3 and MgO," Nature, 188, 43(1960).

19. P.A. Sanger, "Neutron Irradiation Damage to the Metallic Components of UWCTR Magnet System," University of Wisconsin Fusion Design Memo 34, (February 1973).

20. C.D. Bopp and O. Sisman, "Radiation Stability of Plastics and Elastomers," ORNL 1373 (1953).

21. O. Sisman and C.D. Bopp, "Physical Properties of Irradiated Plastics," ORNL 928 (1951).

22. R. Mowers, "Properties of Non Metallic Materials at Cryogenic Temperatures," Proceedings of the 1968 Summer Study on Superconducting Sevices and Accelerators," BNL 50155 (C-55), Volume 1, p. 311.

23. G.J. Dau and M.V. Davis, "The Electrical Conductivity of Alumina at Temperature in Reactor Environment," Nuc. Sci. Eng., 21, 30 (1965).

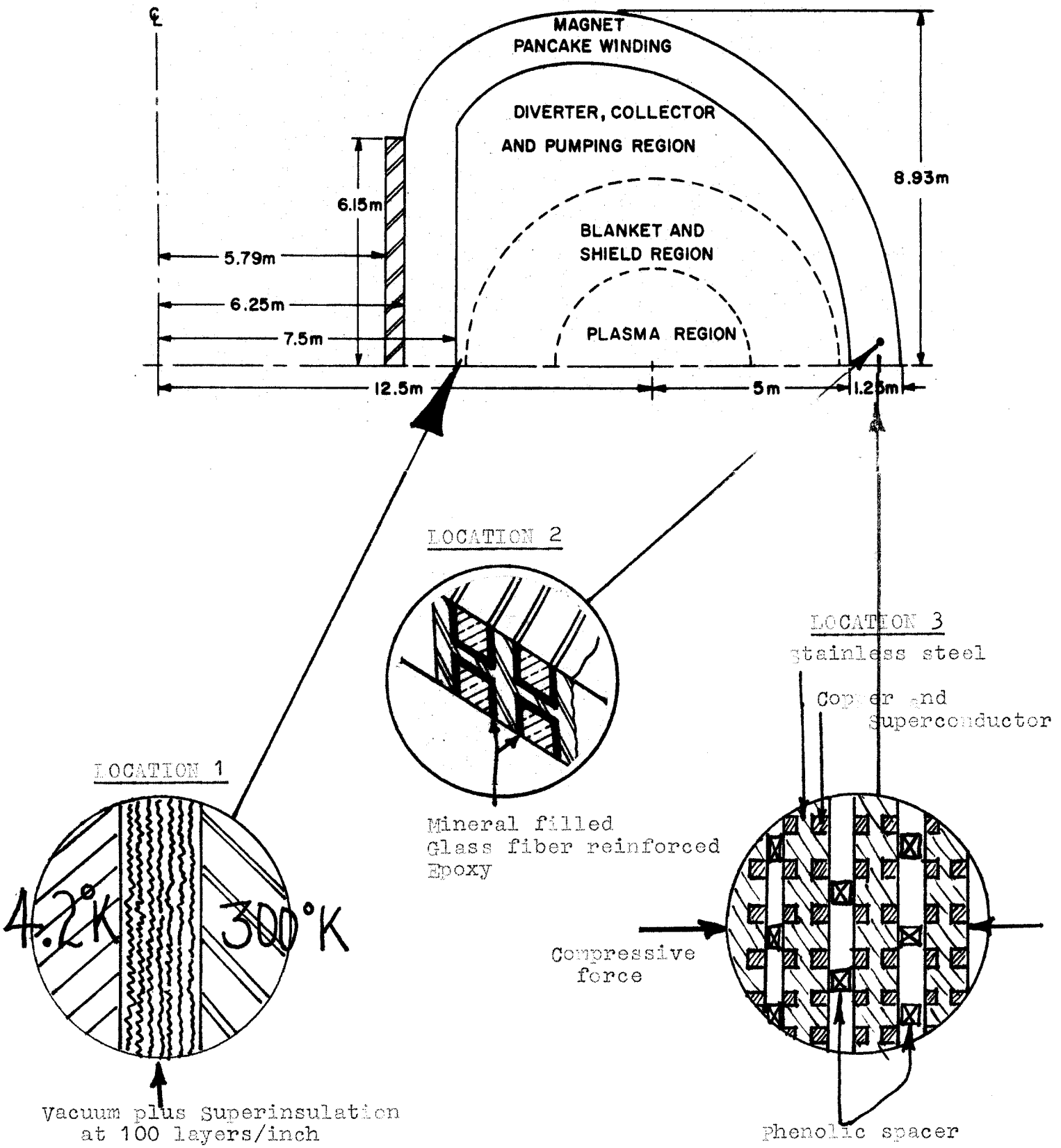

Figure 1 Locations of insulating components in UWCTR magnet.

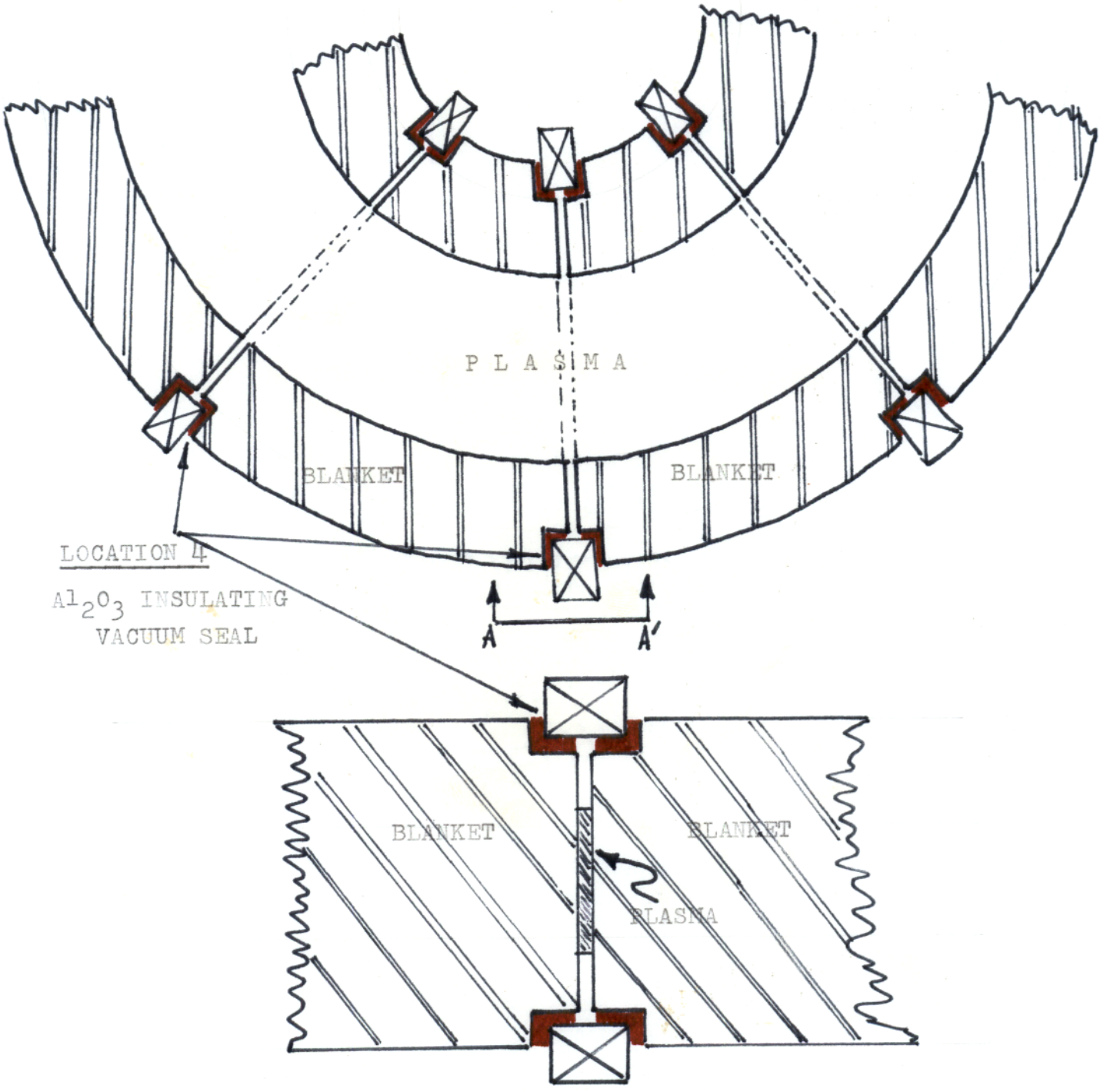

Figure 2 Location of Insulator in the UWCTR Blanket

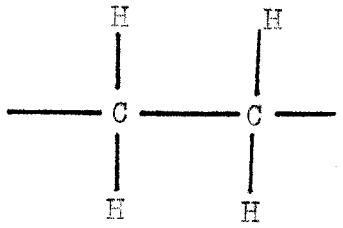

Polyethylene

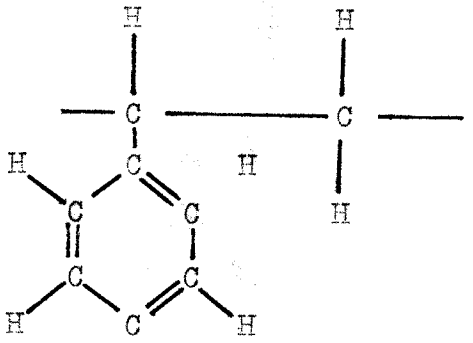

Polystyrene

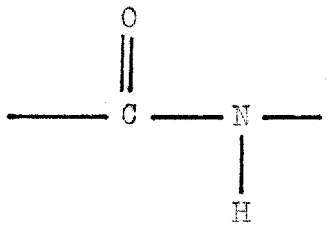

Nylon

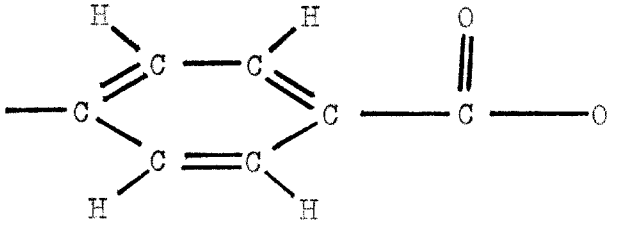

Dacron

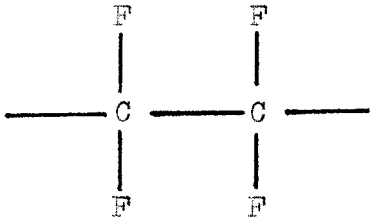

Teflon

Figure 3 Common polymeric materials (Reference 1)

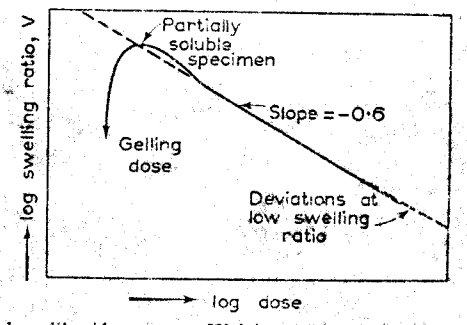

FIG. 9.7. A typical swelling/dose curve. Weight swelling ratio = swollen weight/initial dry weight.

Figure 4. Typical swelling curve for polyethylene[1]

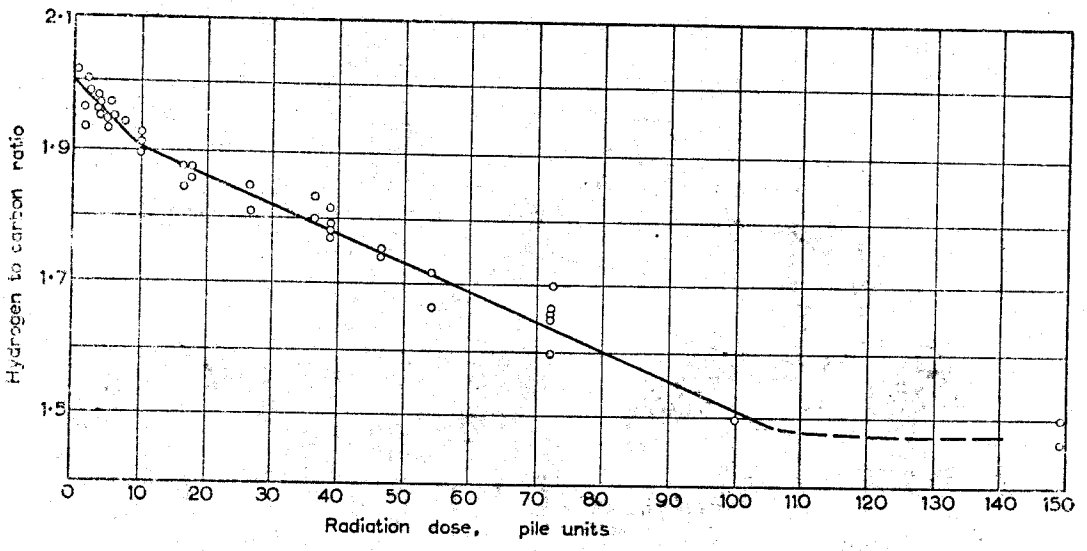

FIG. 13.21. Decrease in hydrogen/carbon ratio in irradiated polyethylene.

Figure 5. Typical decrease of hydrogen curve for polyethylene[1]

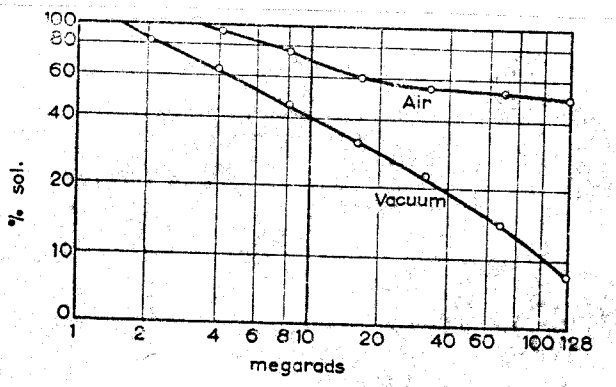

FIG. 13.26. Decrease in sol fraction with electron dose for 18μ specimen irradiated in air or in vacuum.

(From: Alexander and Toms, 1956.)

Figure 6. Effect of oxygen on crosslinking for polyethylene[1]

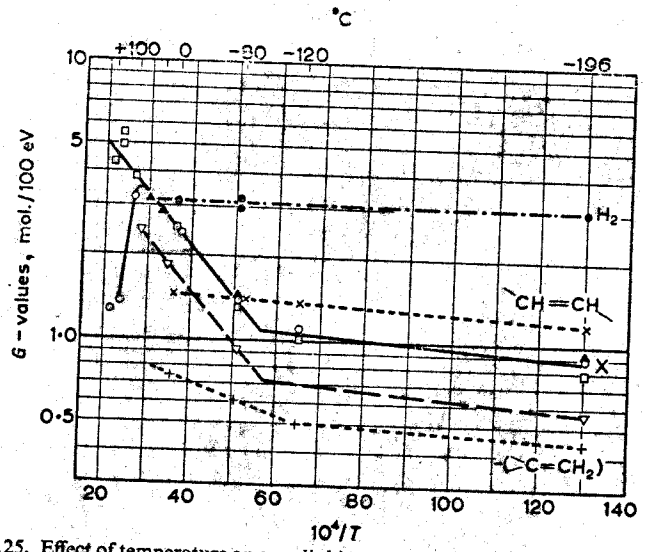

FIG. 13.25. Effect of temperature on crosslinking, unsaturation and hydrogen evolution.

G values are given for hydrogen evolution (●), formation of *trans*-unsaturation (x), and loss of initial unsaturation (+); they were all measured on the same samples (20 megarads).

G values for cross-links X were deduced from elasticity (▲ after correcting for end-effects; 25 and 40 megarads), from swelling (0) and solubility (□) by comparison with the dose required to give the same effect at room temperature and normalized to $G(X) = 2{\cdot}5$ at 0°C (20 megarads).

$G(X)$ values deduced from elasticity measurements for γ-irradiation in air are shown (▽) for comparison, after correcting for $G(\mathrm{Fe}) = 15{\cdot}5$.

Figure 7. Effect of temperature on G-values of polyethylene[1]

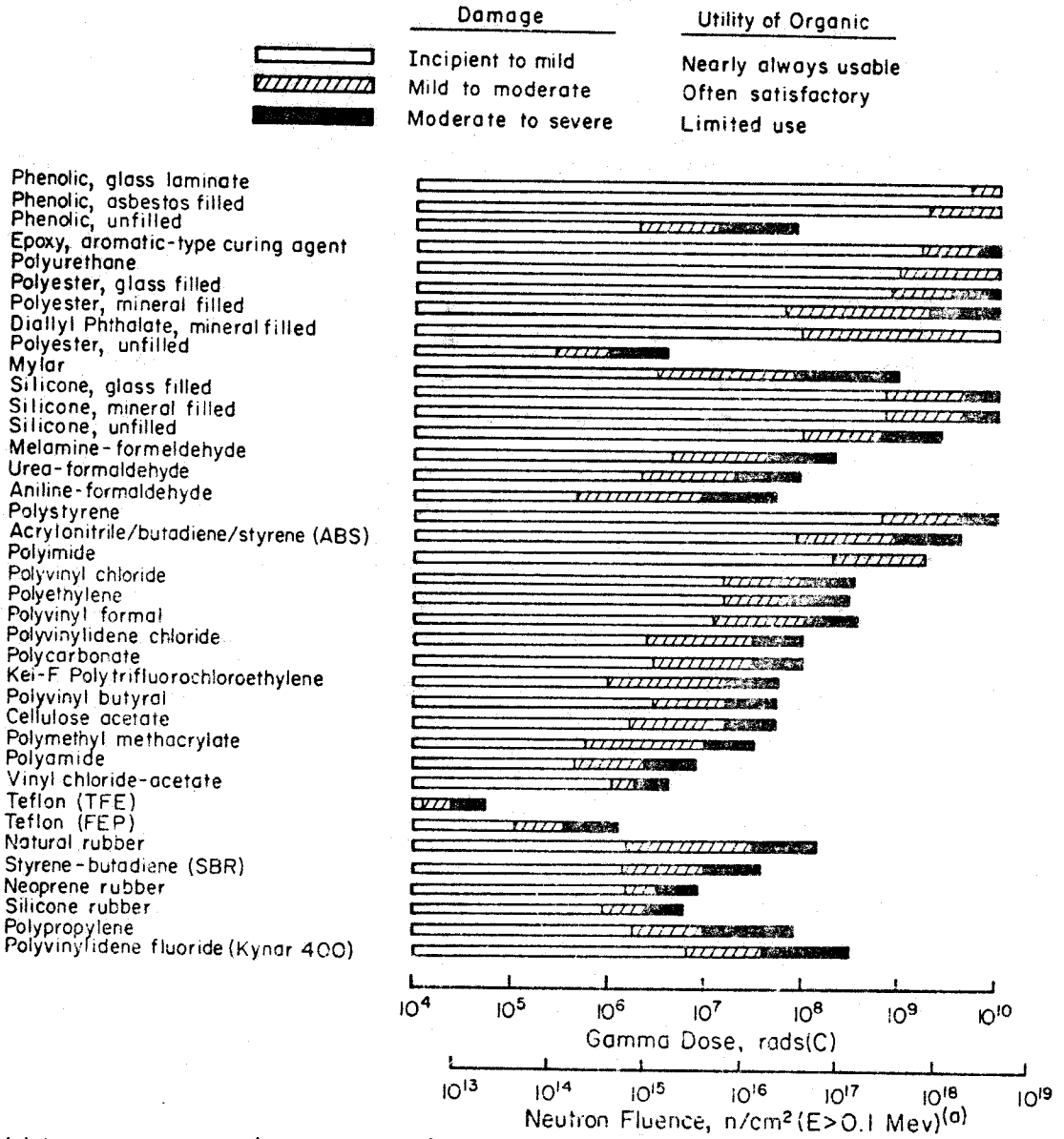

(a) Approximate fluence (1 rad(C) = 4×10^8 n/cm^2)

FIGURE 8. RELATIVE RADIATION RESISTANCE OF ORGANIC INSULATING MATERIALS BASED UPON CHANGES IN PHYSICAL PROPERTIES [3]

A. *Damage to Long Chain Polymers*

Monomer	Type	Dose for damage (megarads) Threshold	Dose for damage (megarads) 25%	Gas evolution ml/g megarad ×10³	Gas evolution μM/g megarad
Methyl methacrylate	Lucite	0·82	11	30	
Tetrafluorethylene	Teflon	0·017	0·037		1·34
Monochlorotrifluoroethylene	Fluorothene	1·3	20		
Styrene	Amphenol	800	4000	0·25	0·011
Styrene α methyl	Q817	4·3	43		
Amide (nylon)	FM.10001	0·86	4·7		
	FM.3003	0·86	4·7	20	0·9
Ethylene terephthalate (Terylene, Dacron)	Mylar	30	120	4	0·18
Ethylene	Polythene	19	93	64	2·85
Vinyl butyral	Butacite	4·7	19		
Vinyl carbazole	Polectron	88	4400		
Vinyl chloride	Geon 2046	19	110		
Vinyl formal	Formvar	16	82	90	4
Vinyl vinylidene chloride	Saran	4·1	45		
Vinyl chloride-acetate	Vinylite	1·4	2·5		

B. *Damage to Formaldehyde Resins*

Formaldehyde	Filler	Type	Dose for damage (megarads) Threshold	Dose for damage (megarads) 25%	Gas evolution ml/g megarad ×10³	Gas evolution μM/g megarad
Aniline	—	Cibanite	0·74	14	6·4	0·3
Melamine	Cellulose	Melmac, Plaskon Melamine	7·4	110	5·4	0 24
Phenol	—	Catalin	2·7	11	3·2	0·14
Phenol	Asbestos fabric	Bakelite	18	770	<0·14	<0·006
Phenol	Asbestos fibre	Bakelite	78	890	<0·14	<0·006
Phenol	Asbestos	Haveg 41	390	3900	<0·14	<0·006
Phenol	Graphite	Karbate	0·89	77	<0·03	<0·013
Phenol	Linen fabric	Bakelite	0·34	2·8	14	0·63
Phenol	Paper laminate	Micarta	0·34	8·2	18	0·8
Phenol	Paper	Bakelite	0·38	26	17	0·76
Urea	Cellulose pulp	Beetle, Plaskon urea	8·3	51	10	0·45

C. *Damage to Miscellaneous Plastics*

Plastic	Type	Dose for damage (megarads) Threshold	Dose for damage (megarads) 25%	Gas evolution ml/g megarad ×10³	Gas evolution μM/g megarad
Allyl diglycol carbonate	CR39	1·5	88	57	2·54
Casein	Ameroid	2·8	27	6	0·27
Furan asbestos + carbon black	Duralon	330	3300	<0·15	<0·006
Polyester	Plaskon alkyd	87	3900	3·1	0·14

D. *Damage to Cellulosics*

Cellulosic	Type	Dose for damage (megarads) Threshold	Dose for damage (megarads) 25%	Gas evolution ml/g megarad ×10³	Gas evolution μM/g megarad
Acetate	Plastacele	2·7	1·9	20	0·9
Acetate butyrate	Tenite II	0·37	7·3	30	1·34
Nitrate	Pyralin	0·63	5·7	130	5·8
Proprionate	Forticel	0·44	4·4	35	1·6
Ethyl	Ethocel	1·4	5·5	31	1·4

FIGURE 9 [ref. 1]

Material and thickness	Dose	Physical properties, original and percent change: Elongation		Tensile		Chemical properties, measured optical densities: Unsaturation			Oxidation		Remarks
	10^6 r.	%	Δ%	p.s.i.	Δ%	Trans	Vinylidene	Vinyl	Carbonyl	Hydroxyl	
Carbonates											
Lexan (0.003 in.)	0	95		6745		—	—	—	0.903	0.129	a
	5		3.1		14.6	—	—	—	0.917	0.125	
	10		−7.4		−2.1	—	—	—	0.920	0.128	b
	50		−22.7		−6.1	—	—	—	0.915	0.154	c
	100		−33.0		−12.9	—	—	—	0.917	0.142	d
	300		—		—	—	—	—	1.020	0.426	e
Macrofol (0.003 in.)	0	75		6795		—	—	—	0.936	0.059	f
	5		6.5		14.6	—	—	—	0.945	0.064	
	10		0.0		−0.1	—	—	—	0.960	0.070	g
	50		−3.9		−2.1	—	—	—	0.979	0.104	h
	100		−28.6		−12.9	—	—	—	1.000	0.150	h
	100-V*		−22.1		−15.7	—	—	—	0.930	0.151	d
Ethylenes											
Alathon 3, NC-10 (0.003 in.)	0	380		1915		—	0.024	—	—	—	i
	5		−3.7		1.1	—	0.019	—	0.040	—	
	10		−7.9		−2.5	0.016	—	—	0.090	—	
	50		−86.8		−33.7	0.027	—	—	0.380	—	j
	100		−95.8		−32.8	0.054	—	—	0.830	—	k
	100-V		−50.0		46.4	0.057	0.013	—	—	—	j
Alathon 3, NC-10 (0.005 in.)	0	510		2330		—	0.047	—	—	—	i
	5		5.1		9.8	0.015	0.038	—	0.060	—	
	10		−3.0		−4.2	0.046	0.030	—	0.140	—	
	50		−84.1		−42.5	0.072	—	—	0.720	—	j
	100		−84.9		−42.7	0.127	—	—	1.250	—	k
	100-V		−67.5		8.2	0.140	0.018	—	—	—	j
Alathon 3, NC-10 (0.010 in.)	0	570		2825		—	0.051	—	—	—	i
	5		3.0		6.5	0.026	0.042	—	0.070	—	
	10		−3.3		−8.2	0.051	0.034	—	0.130	—	
	50		−81.8		−57.2	0.176	—	—	0.740	—	j
	100		−91.6		−57.7	0.173	—	—	1.350	—	k
	100-V		−65.9		1.6	0.240	0.025	—	—	—	j
Alathon 3, NC-10 (0.015 in.)	0	650		2330		—	0.071	—	—	—	i
	5		−10.6		17.8	0.052	0.058	—	0.070	—	
	10		−10.9		22.2	0.088	0.052	—	0.170	—	
	50		−82.7		−42.7	0.285	0.027	—	0.820	—	j
	100		−90.4		−40.2	0.380	—	—	1.500	—	k
	100-V		−73.1		7.1	0.384	0.042	—	—	—	j
Marlex 50 (0.002 in.)	0	600		4280		0.021	—	0.095	0.035	—	i
	5		−91.7		−12.7	—	—	0.067	0.060	—	
	10		−97.8		−35.3	—	—	0.055	0.110	—	
	50		−100.		−100.	0.053	—	—	0.438	—	l
	100		—		—	—	—	—	—	—	m
	100-V		−95.3		−7.5	0.092	—	—	—	—	j
U-101 (0.005 in.)	0	535		2180		0.006	0.045	—	0.029	—	i
	5		−0.6		6.4	0.011	0.031	—	0.047	—	
	10		−10.8		−13.4	0.017	0.021	—	0.136	—	
	50		−81.2		−47.4	0.070	0.017	—	0.788	—	j
	100		−96.6		−46.8	0.076	—	—	1.130	—	k
Polyethylene U-201 (0.005 in.)	0	575		1895		0.011	0.054	—	0.039	—	i
	5		−5.2		5.0	0.017	0.037	—	0.066	—	
	10		−10.8		−4.2	0.019	0.030	—	0.106	—	
	50		−92.5		−35.3	0.059	0.024	—	0.750	—	j
	100		−96.4		−34.2	0.107	0.014	—	1.010	—	k
Irrathene 101 (0.010 in.)	0	525		2390		0.007	0.045	—	0.052	—	i
	5		2.7		9.8	0.083	0.044	—	0.135	—	
	10		−5.2		5.1	0.095	0.043	—	0.215	—	
	50		−68.3		−47.3	0.197	0.036	—	0.755	—	j
	100		−94.4		−44.4	0.212	0.032	—	1.168	—	k
	100-V		−64.8		11.4	0.307	0.028	—	—	—	j
Irrathene 201 (0.010 in.)	0	595		2405		0.008	0.045	—	0.058	—	n
	5		−6.2		13.4	0.078	0.039	—	0.090	—	
	10		−9.4		2.9	0.097	0.035	—	0.177	—	
	50		−69.8		−36.7	0.162	0.036	—	0.625	—	j
	100		−91.5		−46.3	0.259	0.027	—	0.862	—	k

(Continued on opposite page)

Figure 10 A Ref. 4

Figure 10B

Table II: Chemical and physical properties of irradiated plastics (Continued)

Material and thickness	*Dose*	*Physical properties, original and percent change*				*Remarks*
		Elongation		*Tensile*		
	10^6 r.	%	Δ%	p.s.i.	Δ%	
Fluorocarbon						
Teflon 1 (0.010 in.)	0	165		2695		i
	.1		−9.1		−44.6	
	.5		−78.8		−54.8	
	1		−87.0		−59.2	
	5		−100.0		−61.1	e
	5-V		−78.8		−47.7	
Polyester						
Mylar A (0.003 in.)	0	150		20,340		o
	5		0.0		0.0	
	10		−13.3		−6.4	
	50		−20.0		−15.6	
	100		−30.3		−34.1	
	100-V		−23.3		−22.8	
Styrene						
Polyflex (0.002 in.)	0	0		11,270		o
	5		—		−6.4	
	22		—		−15.9	
	55		—		−13.4	
	100		—		−23.2	j
	100-V		—		−25.5	
Vinyl chlorides						
Geon 8630	0	245		2555		p
(0.004 in.)	5		−10.7		−25.6	q
	10		−21.3		−34.5	r
	50		−26.5		−36.2	s
	100		−38.8		−31.5	t
Geon 8630	0	300		2735		p
(0.020 in.)	5		4.0		−5.7	q
	10		4.6		−6.2	r
	50		−19.2		−10.2	s
	100		−28.3		−6.0	t
Geon 8640	0	225		3150		o
(0.004 in.)	5		−8.5		−13.3	u
	10		−11.8		−28.1	v
	50		−44.4		−44.4	w
	100		−46.7		−42.3	x
	100-V		−29.1		−22.4	w
Geon 8640	0	325		3580		o
(0.020 in.)	5		−5.3		−5.1	u
	10		−2.2		−4.1	v
	50		−22.2		−32.0	w
	100		−32.3		−31.2	x

*V- Irradiated in vacuo.
a - Light tan transparent.
b - Light yellow.
c - Light amber.
d - Slightly darker amber.
e - Very [illegible] brittle on bend test; could not test.
f - Light amber transparent.
g - Very slightly darker amber.
h - Darker amber.
i - Off white translucent.
j - Light yellow [illegible]
k - Slightly darker yellow.
l - Quite brittle; broke on bend test.
m - Crumbled; could not test.
n - Discolored [illegible] time.
o - Clear transparent.
p - Transparent, slight cloudiness.
q - Light [illegible]
r - Light [illegible]
s - Dark [illegible]
t - Dark [illegible]
u - Very light amber and opaque.
v - Light brown [illegible]
w - Dark [illegible]
x - [illegible]

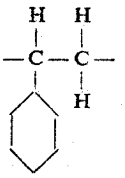

The repeating unit in the structural formula of polystyrene, which is the most stable of the unfilled polymers tested.

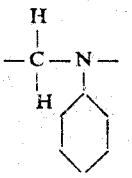

The repeating unit of aniline formaldehyde polymer. As for polystyrene, stability is attributed to the bulky benzene-ring-containing side groups.

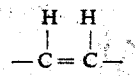

Present in many elastomers; since the stability of elastomers appears to be insensitive to the amount of unsaturation, this group is ranked with next group.

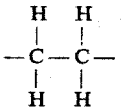

The repeating unit of polyethylene.

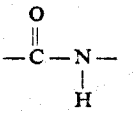

Present in nylon, which shows the same order of stability as polyethylene.

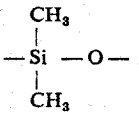

The repeating unit of silicone rubber, which shows the same order of stability as most other elastomers.

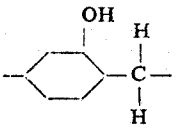

The repeating unit of phenol formaldehyde polymer. Presence of benzene ring in main chain is thought to increase cleavage, since unfilled phenolic crumbles for exposures that do not decrease strength of polyethylene (this contrasts with effect of benzene ring in polystyrene, in which it is in a side group).

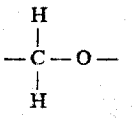

Also taken to be less stable than polyethylene. Polyallyl diglycol carbonate, polyvinyl formal and polyvinyl butyral are softened. Selectron-5038 is hardened; however, this plastic is initially very soft and shows a high rate of crosslinking.

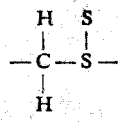

Present in Thiokol, for which a balancing of cleavage against crosslinking causes small hardness change, but decreases the ultimate strength.

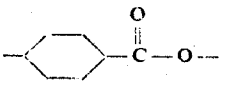

Present in Dacron. The predominant radiation change is embrittlement.

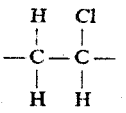

Present in polyvinyl chloride. Unplasticized polyvinyl chloride is softened by cleavage, though highly plasticized forms are hardened.

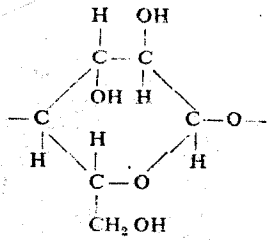

The repeating unit of cellulose. Rapid embrittlement of cellulosic plastics shows that this structure is sensitive to chain cleavage.

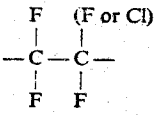

The repeating unit of Teflon and Fluorothene, which become brittle and crumble apart at relatively short exposure. Resistance to cleavage is poor.

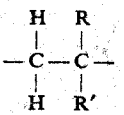

The repeating unit in polymers with quaternary carbon atoms: polymethyl methacrylate, butyl rubber and polyalphamethyl styrene.

Figure 11. Polymer groups ranked in order of stability against cleavage. (Bopp and Sisman, 1955). A different order may be obtained if the assessment is based on other properties such as solvent resistance.

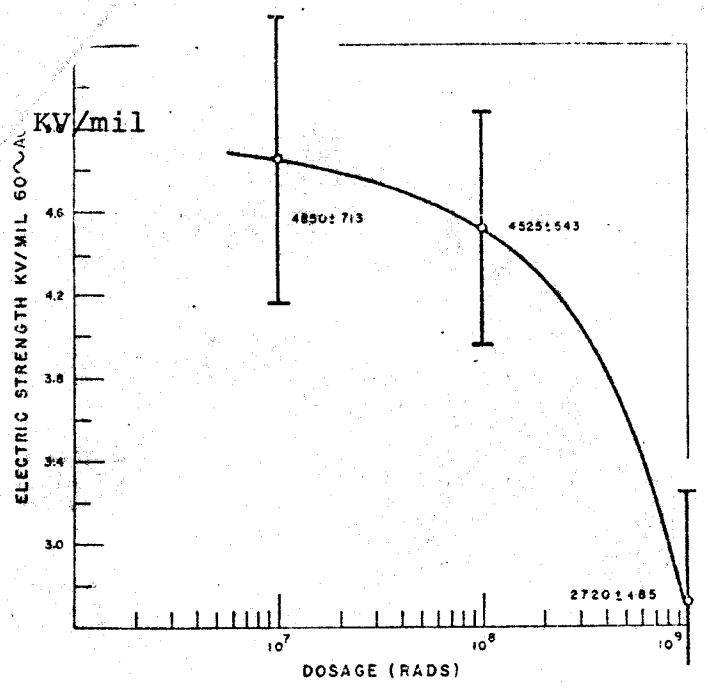

Figure 12. Electric strength as a function of dosage. Rate 10^5 rads/minute

Figure 13 Ref. 9

MECHANICAL, THERMAL AND ELECTRICAL PROPERTIES OF MINERAL FILLED AND GLASS FIBER REINFORCED, CURED THERMOSETTING RESINS

Properties	Epoxies	Silicones (low viscosity)	Polyester (rigid type)
Tensile strength (kg/cm^2)	3900	1500	3200
Young-E-modulus (kg/cm^2)	$(2\text{-}4) \times 10^5$	2×10^5	2.1×10^5
Compression strength (kg/cm^2)	3500	1650	2500
Flexural strength (kg/cm^2)	5700	2850	4100
Impact strength, Izod ($cm \cdot kg/cm$)	80	27	100
Specific gravity (gr/cm^3)	1.6 - 2	1.5 - 1.8	1.9
Specific heat ($Ws/gr.^oC$)	0.8	~ 0.8	≈0.8
Thermal conductivity ($W/cm \cdot ^oC$)	8×10^{-3}	1×10^{-2}	1.1×10^{-2}
Thermal expansion coefficient ($^oC^{-1}$)	$1.3\text{-}1.8 \times 10^{-5}$	$\sim 2 \times 10^{-5}$	1.6×10^{-5}
Maximum heat of operation (^oC)	200	300	200
Heat distortion (^oC)	220	370	220
Volume resistivity ($ohm \cdot cm$)	10^{16}	4×10^{15}	10^{14}
Dielectric strength ($volt \cdot cm^{-1}$)	2×10^5	1.2×10^5	4×10^4
Viscosity at casting temperature (cP)	>1000	>2000	>2000
Shrinkage during cure (%)	0.2	0.1	0.5
Casting temperature (^oC)	60-140	25-30	25-30
Resin content by weight (%)	≈25-30	30-38	30-40
Insulation resistance (MΩ)	20,000	10,000	700

Figure 14 Ref. 9

RELATIVE RADIATION RESISTANCE OF THERMOSETTING RESINS AT ROOM TEMPERATURE

Resin	Radiation dosage ($ergs \cdot gr^{-1}$) required for:			
	threshold damage	25% damage	50% damage	90% damage
Epoxy				
Unfilled[a]	2×10^{10}	3.2×10^{11}	10^{12}	7×10^{12}
Laminated, glass fiber[b]	2.5×10^{11}	2.65×10^{12}	7.4×10^{12}	$\sim 2 \times 10^{13}$
Mineral filled[c]	10^{11}	5×10^{11}	3×10^{12}	$\sim 10^{13}$
Mineral filled and laminated, glass fiber	8×10^{11}	5×10^{12}	1.25×10^{13}	3.5×10^{14}
Polyester				
Unfilled[d]	5×10^{7}	1.2×10^{8}	5×10^{9}	-
Laminated, glass fiber[b]	8×10^{10}	5×10^{11}	10^{12}	-
Mineral filled	9×10^{9}	1×10^{11}	4×10^{11}	-
Silicone				
Unfilled[e]	10^{10}	4×10^{10}	2×10^{11}	-
Laminated, glass fiber[b]	1×10^{11}	10^{12}	6×10^{12}	-
Mineral filled	1×10^{11}	-	-	-

a) Epoxy: DER 332 LC and Epon curing agent Z or curing agent MPDA and MDA.

b) Medium weave, Volan A treated fiberglass.

c) Alumina, 900 mesh.

d) Unsaturated, low pressure, low viscosity polyester resin.

e) Silicone resin: R-7521, curing agent dicumyl peroxide and zircon filler.

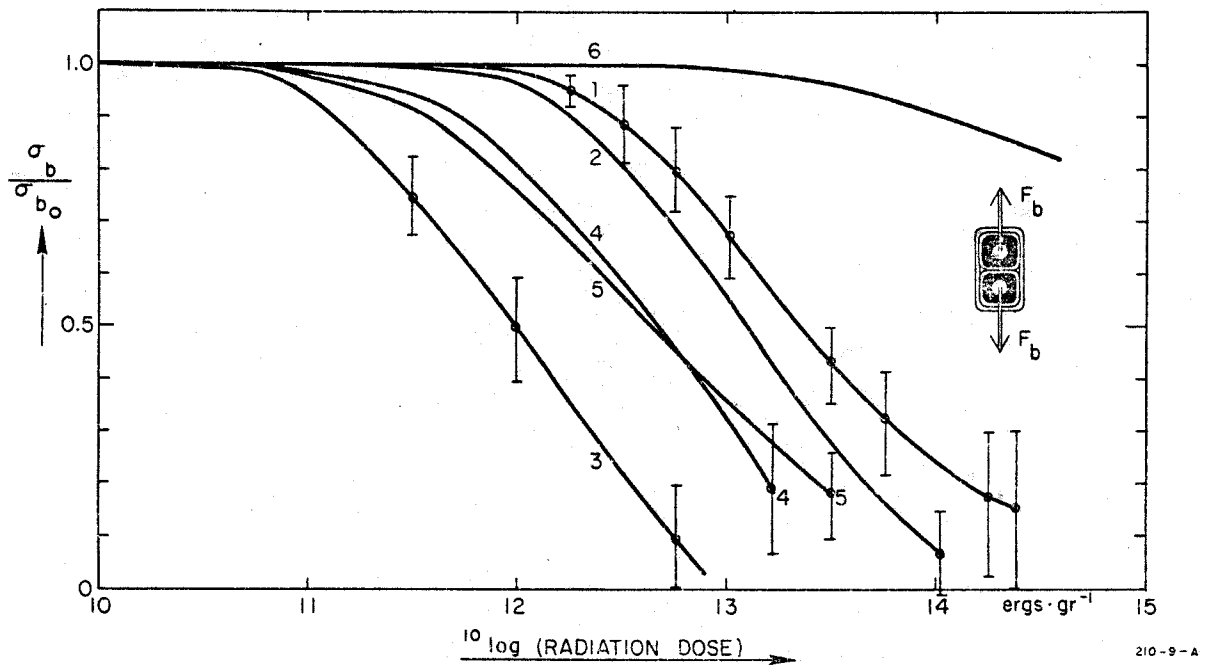

FIG. 15--Bond strength of glass fiber reinforced and mineral-filled thermosettings and ceramica. (1) DER 332 LC and curing agent MPDA and MDA wetting agent Z6040 (σ_{b_i} = 183 kg cm^{-2}); (2) Epon 828/1031 curing agent NMA and BDMA (σ_{b_i} = 189 kg/cm^2); (3) Emerson and Cuming 2850 FT no glass fiber reinforcement (σ_{b_i} = 62 kg cm^{-2}); (4) DER 332 LC and curing agent BF_3MEA (σ_{b_i} = 175 kg cm^{-2}); (5) Dow Corning R-7521 silicone and curing agent dicumyl peroxide; zircon filler (σ_{b_i} = 70 kg cm^{-2}); (6) Eccoceram part A and B (σ_{b_i} = 22 kg cm^{-2}).

Reference 9

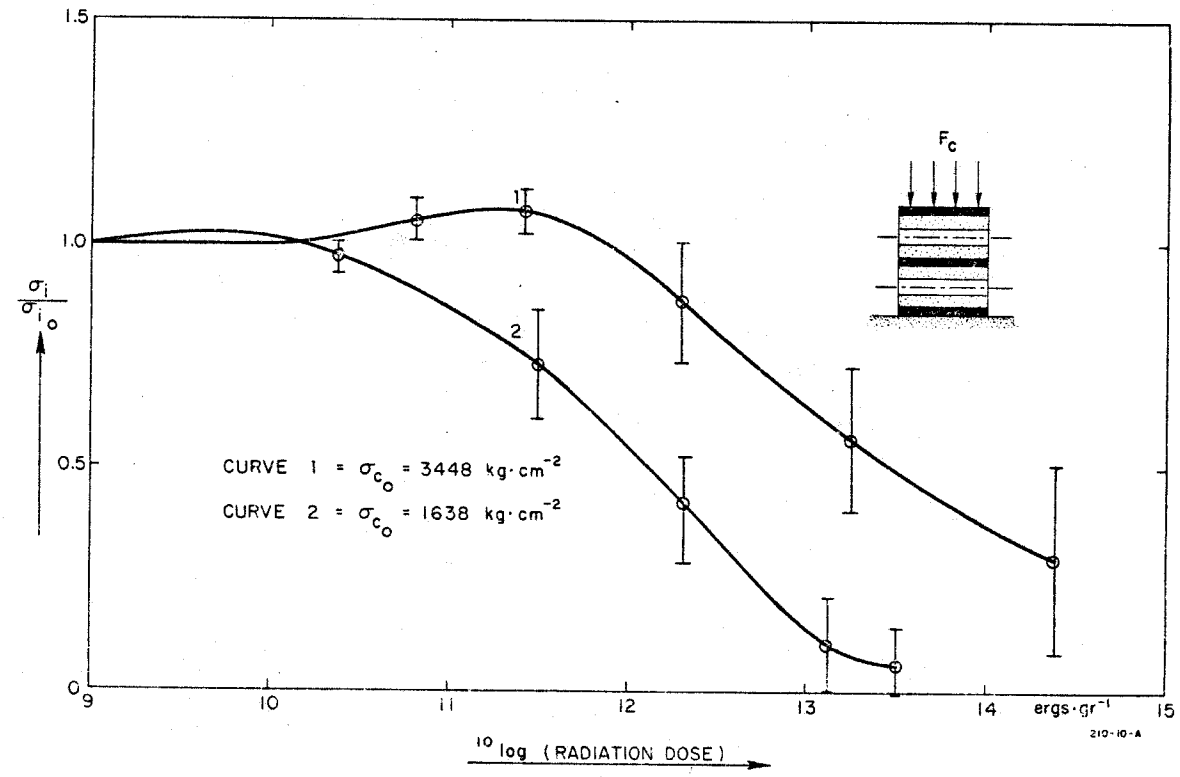

FIG. 16--Relative compression strength of glass fiber reinforced, mineral-filled thermosettings as a function of absorbed radiation dose. (1) DER 332 LC and hardener MPDA and MDA (Al_2O_3 filler); (2) R-7521 silicone resin hardener dicumyl peroxide (zir

(Reference 9)

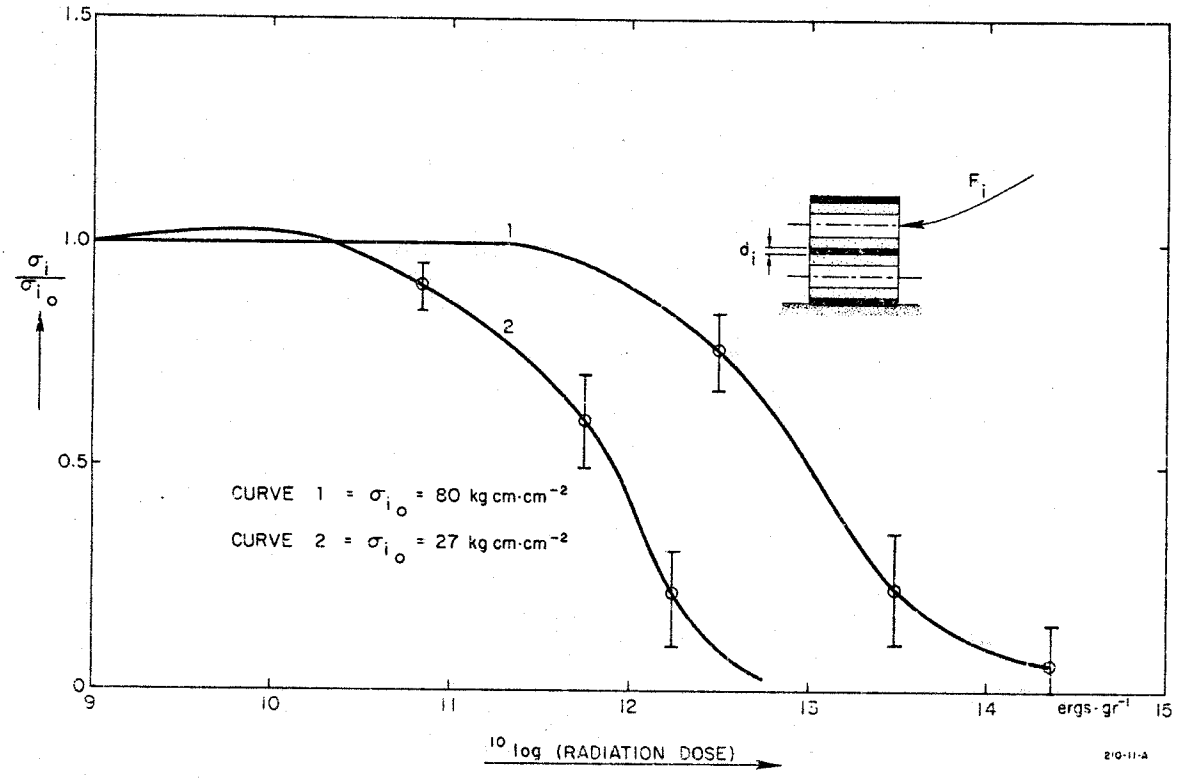

FIG. 17--Relative impact strength of glass fiber reinforced, mineral-filled thermosettings as a function of absorbed radiation dose. (DER 332 LC and MPDA and MDA (Al_2O_3 filler); (2) R-7521 silicone resin (zircon filler).

(Reference 9)

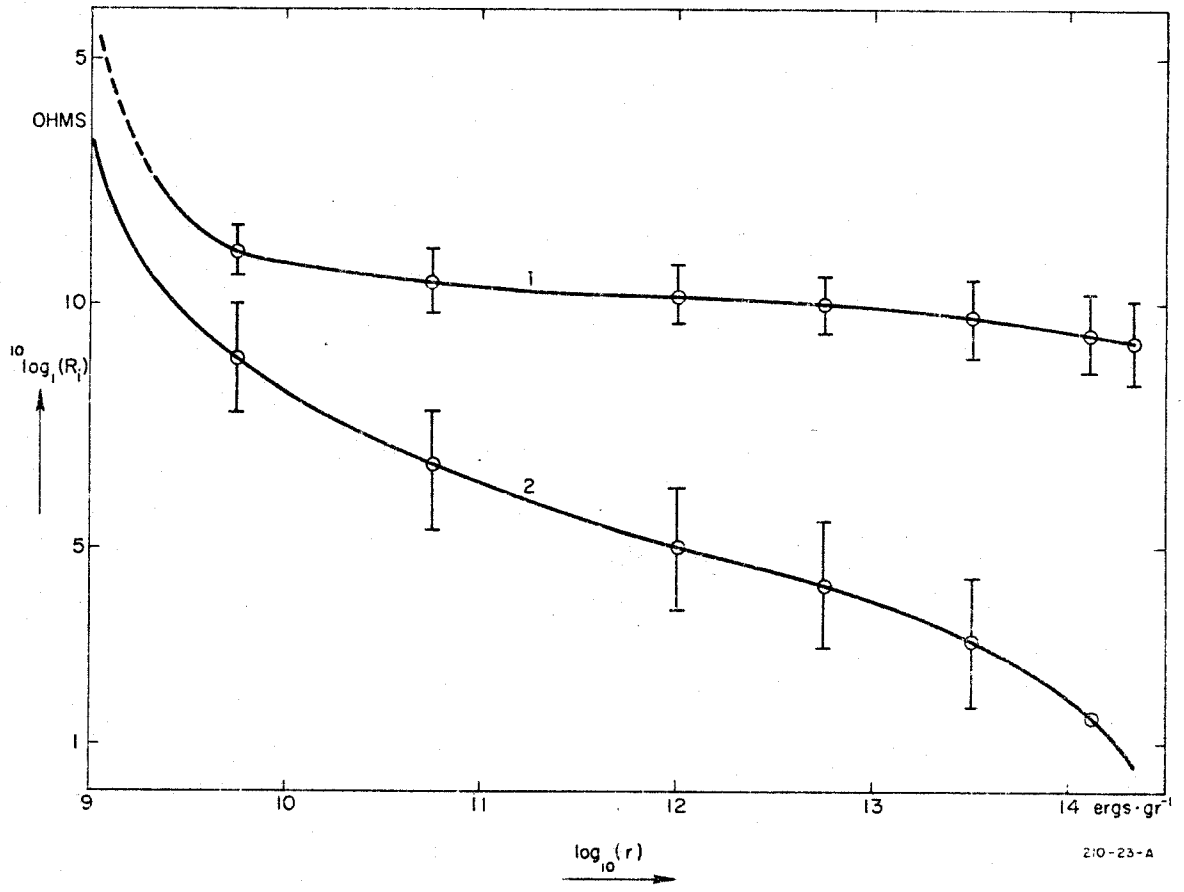

FIG. 18--Insulation resistance of irradiated glass reinforced thermoset according to the following specifications:
Epoxy DER 332 LC hardener MPDA and MDA
Alumina filled and glass reinforced with glass tape
Volan A treated medium weave
Curve 1 dry insulation; curve 2 wetted insulation

(Reference 9)

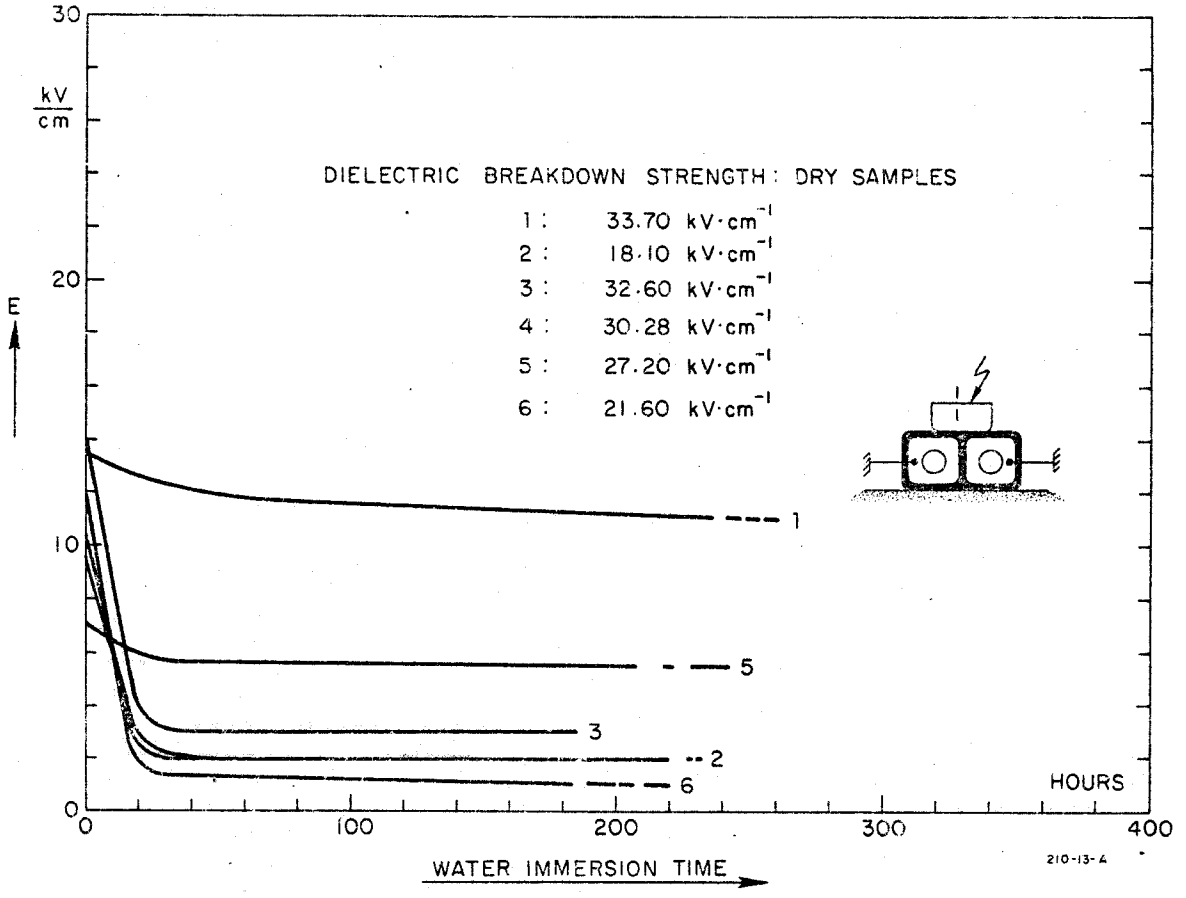

FIG. 19--Corona threshold of nonradiated and irradiated glass fiber reinforced, mineral-filled epoxies. (Samples immersed in 25°C tap water) (1) Nonradiated DER 332 LC and hardener DMA and MPDA; (2) irradiated absorbed dose 5×10^{12} ergs·gr^{-1}(binder as in 1); (3) irradiated absorbed dose 1.09×10^{14} ergs·gr^{-1} (binder as in 1); (4) irradiated absorbed dose 3.25×10^{14} ergs·gr^{-1} (binder as in 1); (5) nonradiated Epon 828/1031 and hardener NMA and BDMA; (6) irradiated absorbed dose 1.19×10^{14} ergs·gr^{-1} (binder as in 5).

(Reference 9)

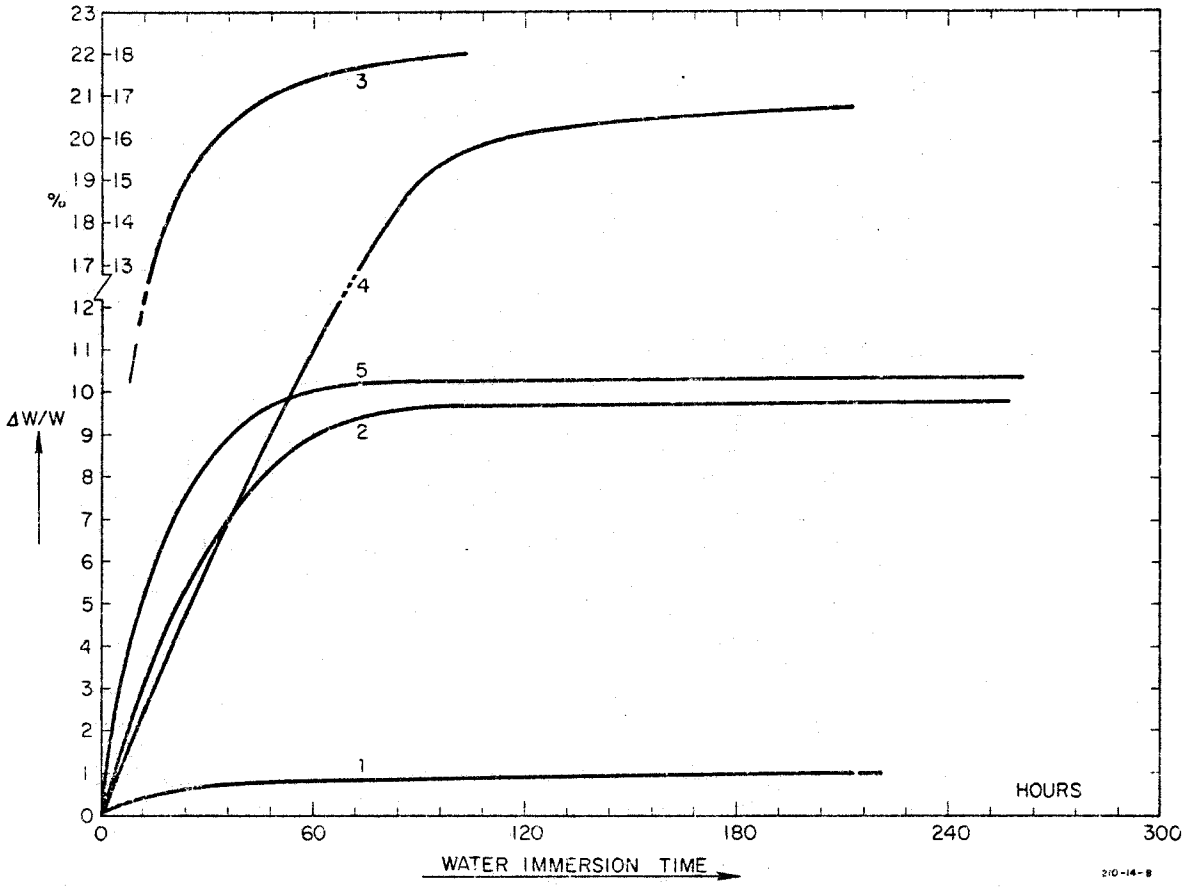

FIG. 20--Moisture absorption of glass fiber reinforced, mineral-filled epoxies of nonradiated and irradiated samples. (Sample immersed in 25°C tap water) (1) Nonradiated. DER 332 LC and hardener DMA and MPDA; (2) absorbed radiation 1.09×10^{14} ergs·gr^{-1} (binder as in 1); (3) absorbed radiation 3.25×10^{14} ergs·gr^{-1} (binder as in 1); (4) absorbed radiation 5×10^{12} ergs·gr^{-1} (binder as in 1). Tests carried on in an LRL pool-type reactor. Samples immersed in water during irradiation; (5) absorbed radiation 1.19×10^{14} ergs·gr^{-1} (binder 2850 FT and hardener 11).

(REference 9)

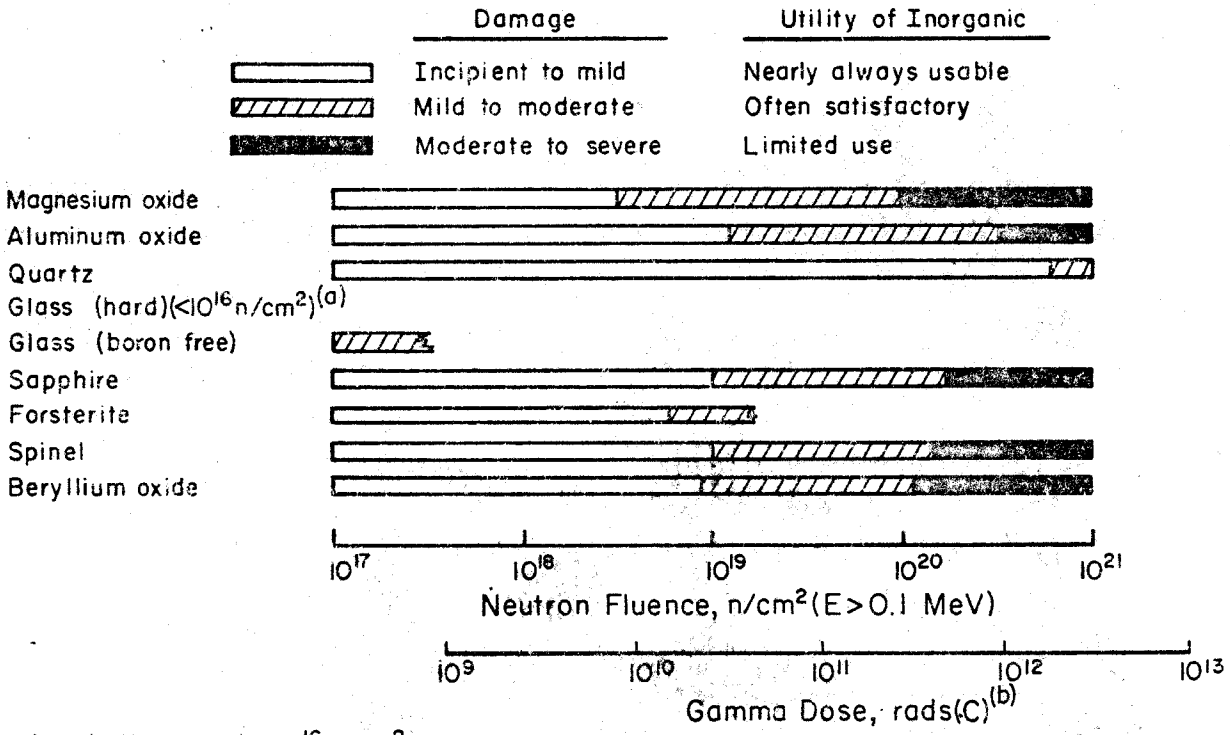

(a) Unsatisfactory at 10^{16} n/cm^2
(b) Approximate gamma dose (4×10^8 n/cm^2 = 1 rad(C))
(c) Varies greatly with temperature

FIGURE 21 RELATIVE RADIATION RESISTANCE(c) OF INORGANIC INSULATING MATERIALS

Based upon changes in physical properties (predominantly elongation) Reference 3)

Property	Type of Oxide	Unirradiated Oxide	Change Due to Irradiation, %	Integrated Flux	Temp. of Irrad., °C	Remarks	Reference
Dimension	Sapphire rod (single crystal)		$< +0.015$	2×10^{19} n cm^{-2}	350		217
Lattice expansion	Synthetic sapphire (single crystal)						
c axis			$+0.01/10^{18}$ n cm^{-2}	2×10^{18} n cm^{-2}	30	At 1.46×10^{19} n cm^{-2}, total expansion along c_o-axis was 0.048% and along a_o-axis was 0.03%. Annealing occurred in two stages, at 300°C and 550°C.	143
a axis			$+0.0061/10^{18}$ n cm^{-2}	2×10^{18} n cm^{-2}			
c axis			$+0.0023/10^{18}$ n cm^{-2}	$(2\text{–}12) \times 10^{18}$ n cm^{-2}			
a axis			$+0.0019/10^{18}$ n cm^{-2}	$(2\text{–}12) \times 10^{18}$ n cm^{-2}			
Lattice expansion	Synthetic sapphire (single crystal)		No change	1.3×10^{8} (1.3 Mev γ) ergs gm^{-1}(C)	−196	No measurable change in physical dimensions although a very pale yellow color was produced in previously colorless crystal.	143
			No change	3×10^{8} (1.3 Mev γ) ergs gm^{-1}(C)			
			No change	2×10^{16} el cm^{-2} (1 Mev)			
			No change	X-ray (50 kv, 80 mA for 5 hr, Cu target)			
Density	Synthetic sapphire (single crystal)		−0.13	1.19×10^{19} n cm^{-2}	<40	Annealing to 400°C resulted in no decrease in the concentration of defects and a steady decrease from 400 to 1250°C. Annealing at 1800°C did not remove coloring, but density returned it to its preirradiation value.	4
Density	Sapphire disk (single crystal)	3.983 g/cc	−0.35	6×10^{19} n cm^{-2} (>100 ev)	~50		57
		3.983 g/cc	−0.98	6×10^{20}	~50		
	Sintered Al_2O_3 disk (polycrystalline)	3.559 g/cc	−0.17	3×10^{19}	~50		
		3.559 g/cc	+6.8	4×10^{20}	~50		
Lattice expansion	Sapphire (single crystal)						
a axis			+0.3	6×10^{20} n cm^{-2}	~30	Significant lattice parameter shifts occurred but diffraction patterns showed that a high degree of perfection was retained.	20
c axis			+0.45				
Lattice expansion	Sintered Al_2O_3 (polycrystalline)						
a axis		4.78 Å	No change	1.6×10^{19} n cm^{-2}	100		212
c axis		12.99 Å	+0.08				
Lattice expansion							
a axis	Al_2O_3 with 0.15% Li_2O		+0.20	1.8×10^{20} n cm^{-2}	~30	Experiment designed to evaluate effect of $Li^6(n, \alpha)H^3$ reaction. X-ray diffraction pattern remained sharp following irradiation.	20
c axis			+0.21				
Thermal conductivity	Synthetic sapphire	60 w/cm deg (at 40°K)	−55	1.5×10^{17} n cm^{-2}		Temperature-independent thermal resistance proportional to dose at low doses, but constant of proportionality decreases at higher doses, i.e., slight saturation effect. Gamma irradiation produced similar initial changes in thermal conductivity, but saturation occurred.	16
			−80	8.9×10^{17}			
			−87	2.0×10^{18}			
			−97	5.0×10^{18}			
		~150 w/cm deg (at 40°K)	~−50	~3×10^{8} ergs gm^{-1}(C) (1.0- and 1.4-Mev gamma rays)			
			~−50	~6×10^{8}			
			~−50	~9×10^{8}			
Thermal conductivity	Sapphire		−50	6×10^{19} n cm^{-2} (>100 ev)	~50		57
	Sintered Al_2O_3		−67	6×10^{20}	~50		
			−42	3×10^{19}	~50		
			−78	4×10^{20}	~50		
Electrical resistivity	Sapphire (single crystal)		−15 to 20	1×10^{9} ergs gm^{-1}(C) (2.5-Mev Van de Graff)	30	After 24 hours at 30°C, about 50% of resistance decrease regained; after 7 days, 100%.	100
	amorphous Al_2O_3		~−5	2×10^{7} ergs gm^{-1}(C) (2.5-Mev Van de Graff)	30		
Electrical resistivity	Three grades of Al_2O_3	2×10^{14} ohm-cm	Decrease by factor of 100	2×10^{19} n cm^{-2}	250	Change due to irradiation not detrimental for resistance less than 1 megohm.	36

Figure 22 Summary of radiation effects to Alumina up to 1964. The references listed are those of reference 2 page 393.

Property	Type of Oxide	Unirradiated Oxide	Change Due to Irradiation, %	Integrated Flux	Temp. of Irrad., °C	Remarks	Reference
Electrical resistance	Polycrystalline Al_2O_3 in powder and disk form	$\sim 10^{10}$ ohms	Decrease to $\sim 10^{8}$ ohms during irradiation	3.5×10^{18} n cm^{-2}	400	Al_2O_3 becomes so highly conducting in a nuclear reactor field that the resistance is essentially independent of temperature. Radiation as well as elevated temperature causes gradual increase in resistivity with time.	153
Electrical insulation in thermocouples	Highly purified Al_2O_3 (polycrystalline)		Loss of some of the insulation properties	5.2×10^{20} n cm^{-2}	400	A high instantaneous neutron flux has no significant effect on insulation properties. Some loss in insulation develops during irradiation occurring rapidly at first, then leveling off to a value still high enough not to effect the operation of the thermocouple.	166
Electrical properties	Polycrystalline Al_2O_3		No change	3.5×10^{11} n cm^{-2}	75	No change found in dielectric constant, dissipation factor, d-c volume resistivity and surface resistivity.	138
Electrical resistance	Polycrystalline	$\sim 10^{12}$ ohms	Decrease to $\sim 10^{7}$ ohms during irradiation	300 micro-amp for 300 sec (500-ev hydrogen ions)		No sign of the observed effect becoming saturated within time scale used. After bombardment, resistance recovered to original value at room temperature with activation energy of ~0.1 ev.	98
Dielectric strength	98% Al_2O_3 + 2% SiO_2	1.4×10^{4} volts/mil	Decrease by a factor of 200	10^{11} ergs gm^{-1}(C) (gamma)	50	Preliminary data. No further results reported.	130
Internal friction	Sapphire (single crystal)		No change	1.6×10^{20} n cm^{-2} (>100 ev)	~50		29
	Sintered (polycrystalline)		No change	1.6×10^{20} n cm^{-2}	~50		
Young's modulus	Al_2O_3 (single crystal)		< −10	$3–6 \times 10^{19}$ n cm^{-2} (>100 ev)	~50		57
			< −10	1.6×10^{20} n cm^{-2}	~50		
	Al_2O_3 sintered		< −10	$3–6 \times 10^{19}$ n cm^{-2}	~50		
			< −10	1.6×10^{20} n cm^{-2}	~50		
Transmission	Sapphire		No loss in transmission	3×10^{12} protons cm^{-2} (19 Mev)		At least 3×10^{13} protons cm^{-2} (19 Mev) required for a 25% loss in transmission in the spectral range to which solar cell used was sensitive.	8
Paramagnetic resonance	α-Al_2O_3		No change	1.5×10^{8} ergs gm^{-1}(C) (γ)	30	Crystal acquired light smoky coloring. After several months at room temperature, color centers annealed out.	93
Color centers	Synthetic sapphire (single crystal)		Increase by a factor of 2	2.9×10^{12} n cm^{-2}	70	To remove all the reactor induced coloring need to heat to 750°C. Large fraction of induced coloring annealed below 730°C.	136
	Al_2O_3 (corundum)		Increase by a factor of 2				
Color centers	Al_2O_3 (corundum)		Slight change	Gamma radiation	70	Study of mechanism of radiation damage.	133
Ceramic to metal seals							
Al_2O_3 to 0.42 Ni − 0.58 Fe	Polycrystalline Al_2O_3		Remained intact	7×10^{20} n cm^{-2}		Work is directed towards producing seals operable at 1200°C.	94
Al_2O_3 to 0.46 Ni − 0.53 Fe			Remained intact	7×10^{20} n cm^{-2}			
Al_2O_3 to 0.51 Ni − 0.49 Fe			Remained intact	7×10^{20} n cm^{-2}			
Al_2O_3 to Fe, Mo, Nb, Zr, Ta			Remained intact	7×10^{20} n cm^{-2}			
Magnetic susceptibility	Polycrystalline Al_2O_3		No change	0.51×10^{19} n cm^{-2} (>0.5 Mev)	30		146
			No change	3.76×10^{19} n cm^{-2} (>0.5 Mev)			

Figure 23. Same as figure 22

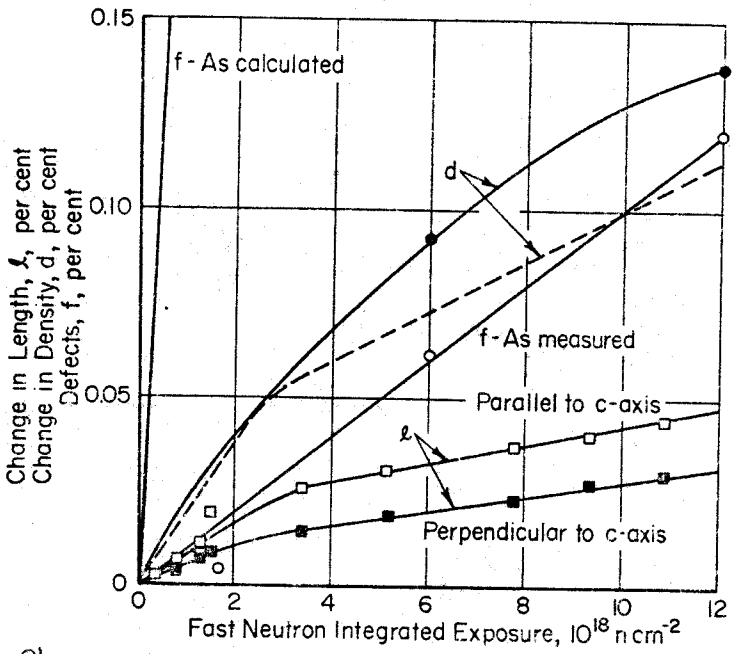

Figure 24. Density changes and defect production in fast-neutron irradiation of α-Al_2O_3[13].

(Reference 2)

Property	Type of Oxide	Unirradiated Oxide	Change Due to Irradiation, %	Integrated Flux	Temp. of Irrad., °C	Remarks	Reference
Density	Single crystal		−0.1 −0.2	$5 \times 10^{19}\ (nv_0)t$ 1.2×10^{21}			42
Density			−0.11	2.2×10^{20}			171
Lattice expansion	Single crystal		+0.17	1.8×10^{20} n cm^{-2}	~30		20
X-ray pattern			No change	1×10^{20} n cm^{-2} (>100 ev)			160
Lattice expansion			+0.038	$2.2 \times 10^{20}\ (nv_0)t$			171
Electrical resistance	Polycrystalline	~7×10^{11} ohms	Decrease to ~10^5 ohms during irradiation	300 micro-amp for 300 sec (500-ev hydrogen ions)		No sign of the observed effect becoming saturated within time scale used. After bombardment, resistance recovered to original value at room temperature with activation energy of ~0.1 ev.	98
Electrical resistivity	Powder		No change	3.5×10^{18} n cm^{-2}	400	There was also an associated gamma flux of 1.4×10^{18} photons cm^{-2}.	153
Electrical capacitance	Powder		No change				
Thermal conductivity			−40	3×10^{19} n cm^{-2} (>100 ev)	~50		28

Figure 25 Summary of radiation effects to MgO up to 1964 Reference numbers listed are found in reference 2 page 393.

Property	Type of Oxide	Unirradiated Oxide	Change due to Irradiation, %	Integrated Flux	Temp. of Irrad., °C	Remarks	Reference
Dimension	Hot-pressed 2.9 g/cc		None	1.4×10^{20} n cm^{-2}	722		142
Linear expansion	2.6 g/cc		+0.01	1×10^{20} n cm^{-2}		Annealed in range 850–1500°C	41
Linear expansion	Hot-pressed 2.8 g/cc		+0.003	2×10^{18} n cm^{-2}	~100	Various reactor facilities used, thus giving different neutron-flux spectra. The resonant frequency had a maximum increase of 0.2%. No evidence of bubble formation in specimens from which residual water had been removed prior to irradiation.	45
			+0.006	4×10^{18}			
			+0.009	6×10^{18}			
			+0.014	1×10^{19}			
			+0.021	1.5×10^{19}			
	2.0 g/cc		+0.005	2×10^{18}			
			+0.010	4×10^{18}			
			+0.016	6×10^{18}			
			+0.021	1×10^{19}			
			+0.040	1.5×10^{19}			
Linear expansion	2.62 g/cc		+0.048	2.5×10^{19} n cm^{-2}	<100	Annealing of (A) specimen for 3 hours produces ~2.5% recovery at 400°C, ~12% recovery at 800°C, and ~38% recovery at 1000°C. Annealing of (B) specimen for 3 hours produces ~8% recovery at 400°C, ~24% recovery at 800°C, and ~58% recovery at 1000°C.	77
	2.75		+0.057				
	2.93		+0.080				
	3.06		+0.096				
	2.70 (B)		+0.110	6×10^{19} n cm^{-2}			
	2.73		+0.139				
	2.90		+0.130				
	3.00 (A)		+0.250				
	3.01		+0.256				
	2.73		+0.304	9×10^{19} n cm^{-2}			
	3.00		+0.655				
Linear expansion	Hot-pressed 2.9 g/cc		+0.7	1.4×10^{20} n cm^{-2}	722		188
			+0.11	1.1×10^{20}	219		
			+0.37	3.5×10^{20}	500		
			+0.06	1.1×10^{20}	458		
			+0.21	3.1×10^{20}	858		
			+0.37	4.5×10^{20}	1025		
			+0.80	4.4×10^{20}	120		
			+2.16	1.8×10^{21}	120		
Linear expansion (continued)	Isostatically pressed 2.7 g/cc		+2.13	2.3×10^{21} n cm^{-2}	120		
			+1.87	2.4×10^{21}	120		
			+0.77	1.1×10^{21}	494		
			+0.63	1.6×10^{21}	737		
			+0.37	2.1×10^{21}	827		
			+2.6	2.3×10^{21}	944		
			+1.4	2.1×10^{21}	950		
Linear expansion	2.7 g/cc		+0.04	3×10^{19} n cm^{-2}	~40		92
			+0.02	7×10^{19}			
			+0.01	1.2×10^{20}			
	2.9 g/cc		+0.03	3×10^{19}			
			+0.04	7×10^{19}			
			+0.03	1.2×10^{20}			
Lattice expansion a-axis			+0.007	6×10^{18} n cm^{-2}	~100	(See dimension)	45
			+0.009	1×10^{19}			
			+0.018	1.5×10^{19}			
			+0.022	6×10^{18}			
c-axis			+0.029	1×10^{19}			
			+0.55	1.5×10^{19}			
Lattice expansion a-axis			+0.011	2.5×10^{19} n cm^{-2}	<100	Specimen (3.0 g/cc) irradiated to 2.5×10^{19} n cm^{-2} at <100 C recovers 46% of lattice expansion after 1 hour at 800°C. A less dense specimen (2.6 g/cc) with same irradiation dose recovers only 54% after 8 hours at 1100°C. Complete recovery occurs after 1–2 hours at 1200–1300°C.	77
			+0.036	6×10^{19}			
			+0.037	9×10^{19}			
			+0.036	2.2×10^{20}	>350		
c-axis			+0.095	2.5×10^{19}	<100		
			+0.31	6×10^{19}			
			+0.52	9×10^{19}			
			+0.256	2.2×10^{20}	>350		

Figure 26 Summary of radiation effects to BeO up to 1964 Reference numbers listed are found in reference 2 page 393

Property	Type of Oxide	Unirradiated Oxide	Change due to Irradiation, %	Integrated Flux	Temp. of Irrad., °C	Remarks	Reference
Thermal conductivity	2.7 g/cc		$R_i/R_o = 1.19$	3×10^{19} n cm^{-2}	40	R_i = Irradiated BeO thermal resistance.	92
			$R_i/R_o = 1.54$	7×10^{19}			
			$R_i/R_o = 1.51$	1.2×10^{20}			
	2.9 g/cc		$R_i/R_o = 1.33$	3×10^{19}		R_o = Unirradiated BeO thermal resistance.	
			$R_i/R_o = 1.46$	7×10^{19}			
			$R_i/R_o = 1.62$	1.2×10^{20}			
Thermal conductivity (at 100°C)			−13	5×10^{20}	185	Complete recovery occurs at 350°C.	147
Rupture modulus	2.8 g/cc	1.94×10^4 lb/in.^{2}	No change	6×10^{18} n cm^{-2}		(See dimension)	45
			+8.3	1×10^{19}			
			+23.7	1.5×10^{19}			
Modulus of elasticity at 20°C	2.74 g/cc		−50	6×10^{19}			
	2.90 g/cc		−64	6×10^{19}	< 100		76
Modulus of elasticity at 20°C	2.62 g/cc		−19	2.5×10^{19}	< 100		
	2.74 g/cc		−40	2.5×10^{19}			
Compressive strength	2.97–3.09 g/cc	20 tons/cm^2 at 20°C	−23 to 57	2.5×10^{19} n cm^{-2}	100		77
			−78	6×10^{19}			
			−93	9×10^{19}			
			powder	2×10^{20}			
			−74	2.2×10^{20}	350		
	2.80 g/cc		−98	2×10^{20} n cm^{-2}	< 100		
	2.74		−93	2×10^{20}			
	2.52		−95	2×10^{20}			
	2.53		−97	3×10^{20}			41
Lattice expansion a-axis	Hot-pressed 2.9 g/cc		+0.011	3.1×10^{20} n cm^{-2}	858		188
			+0.011	4.5×10^{20}	1025		
			+0.078	4.4×10^{20}	120		
			+0.019	1.1×10^{21}	494		
			+0.015	1.6×10^{21}	737		
			+0.015	2.1×10^{21}	827		
			+0.015	2.6×10^{21}	900		
			+0.022	2.1×10^{21}	950		
c-axis			+0.16	3.1×10^{20} n cm^{-2}	858		
			+0.091	4.5×10^{20}	1025		
			+0.523	4.4×10^{20}	120		
			+0.182	1.1×10^{21}	494		
	Isostatically pressed 2.7 g/cc		+0.137	1.6×10^{21} n cm^{-2}	737		
			+0.137	2.1×10^{21}	828		
			+0.114	2.6×10^{21}	900		
			+0.137	2.1×10^{21}	950		
Lattice expansion a-axis			+0.03	7×10^{20} n cm^{-2}			7
c-axis			+0.09				
Thermal conductivity	2.84 g/cc		−30	7×10^{19} n cm^{-2} (> 100 ev)			57
Thermal conductivity (at 140°C)	2.74 g/cc (C)		−14	2.5×10^{19} n cm^{-2}	< 100	Annealing of (C) for 5 hours at 500°C produces ~40% recovery, whereas similar treatment of (D) produces ~33% recovery.	77
			−69	6×10^{19}			
	3.00 g/cc (D)		−32	2.5×10^{19}			
			−80	6×10^{19}			

Figure 26 continued

Property	Type of Oxide	Unirradiated Oxide	Change due to Irradiation, %	Integrated Flux	Temp. of Irrad., °C	Remarks	Reference
Compressive strength	2.9 g/cc		+9	1.3×10^{20} n cm^{-2}			76
Compressive strength			+14 +14 +16	3×10^{19} n cm^{-2} 7×10^{19} 1.2×10^{20}	~40		92
Tensile strength	Hot pressed 2.7-3 g/cc		−10	2.5×10^{19} n cm^{-2}	<100		76
Strength	Hot-pressed at 1750°C and 2400 psi		Specimens disintegrated under thermal cycling	3×10^{20} n cm^{-2}	<100		
Mechanical integrity	Hot-pressed 2.9 g/cc		None	1.4×10^{20} n cm^{-2} 0.8×10^{20} 2.9×10^{20} 1.1×10^{20} 2.9×10^{20}	722 219 500 458 858		115
			3 radial cracks None	4.4×10^{20} 3.7×10^{20}	1025 120		
	Cold-pressed and sintered at 1450°C		Cracking and powdering, various degrees		120		
	2.6 g/cc		None One crack Radial cracks Gross cracking Gross cracking Gross cracking and powdering Gross powdering	1×10^{21} n cm^{-2} 1×10^{21} 1×10^{21} 1×10^{21} 1×10^{21} 1×10^{21} 1×10^{21}	444 737 827 900 944 950 110		
Stored energy			None released up to 500°C	5×10^{19} n cm^{-2}			41

Figure 26 continued

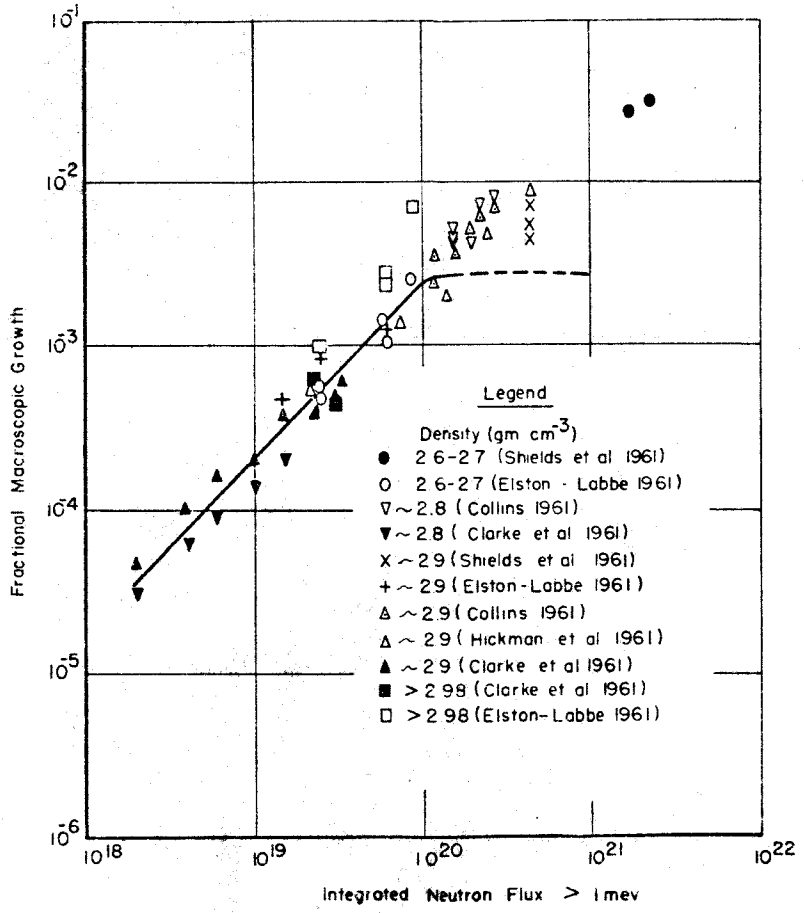

A. Fractional macroscopic growth in beryllium oxide specimens of various densities as a function of neutron dose. The continuous line represents the theoretical growth, g_T, obtained from lattice expansion data. The irradiation temperatures were between 80 and 170°C[46].

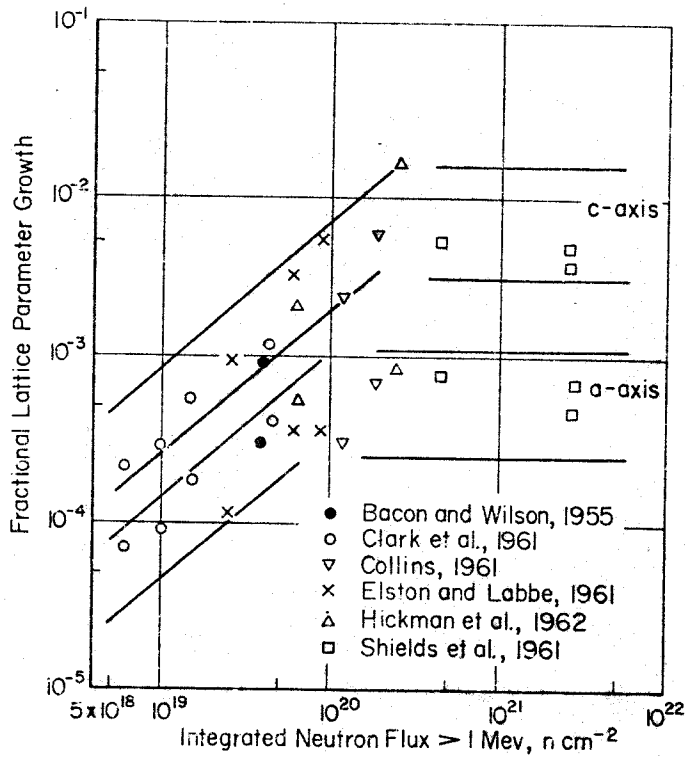

B. Change of c- and a-parameters in irradiated beryllium oxide as a function of neutron dose at 70 to 150°C irradiation temperature[46].

FIGURE 27 Ref. 2

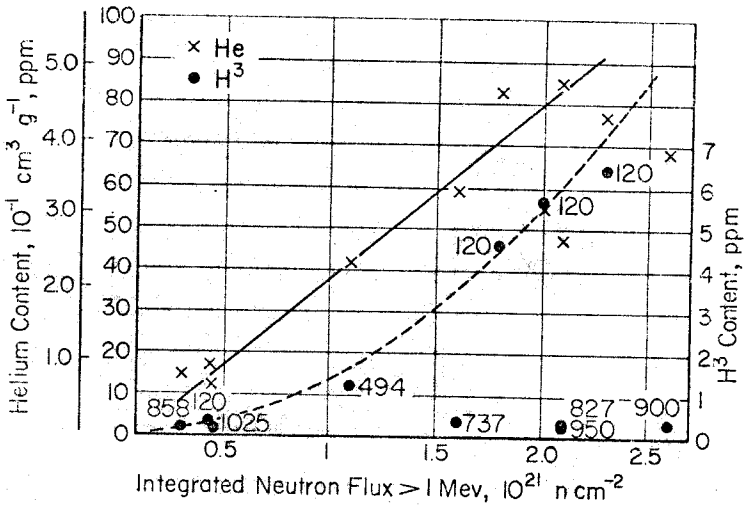

Figure 6.15. Helium and tritium content of irradiated beryllium oxide as a function of neutron dose and for tritium at various irradiation temperatures[188].

Figure 28 Reference 2

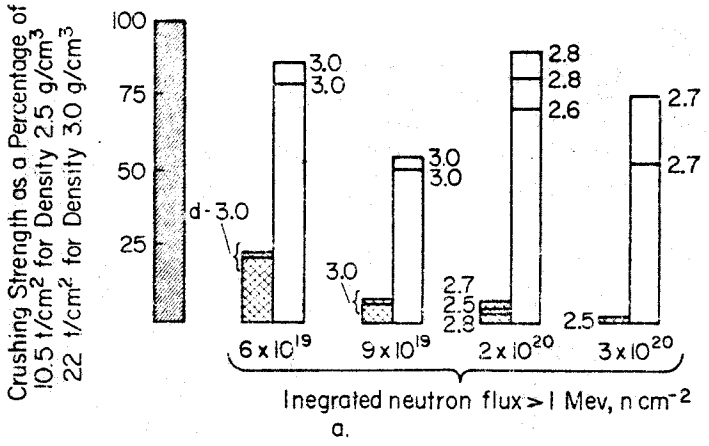

Figure 6.12a. Crushing strength for 100°C irradiations, as a function of neutron dose and sample density (left-hand column), and the restoration of strength obtained by annealing for 24 hours at 1300°C (right-hand column.) — Strength level for each sample measured[77].

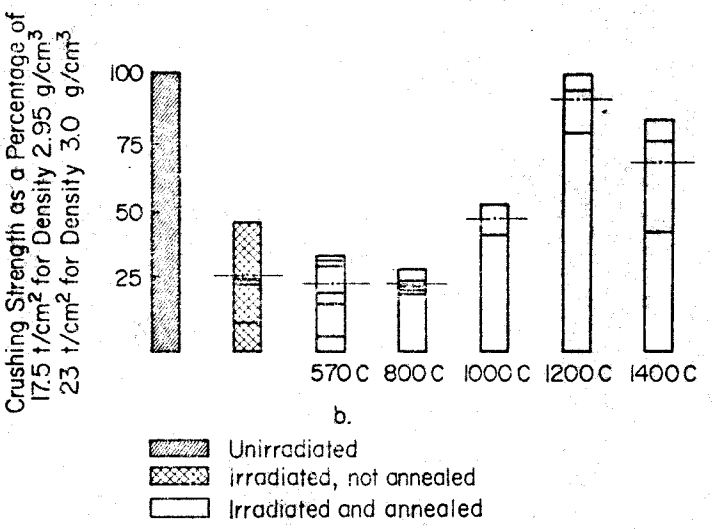

Figure 12b. Crushing strength for 350°C irradiations to a dose of 2×10^{20} *n/t* for 2.95–3.00 g cm^{-3} samples and the restoration of strength obtained by annealing. — strength level for each sample measured — · — mean of results in each column.

Figure 29. Reference 2

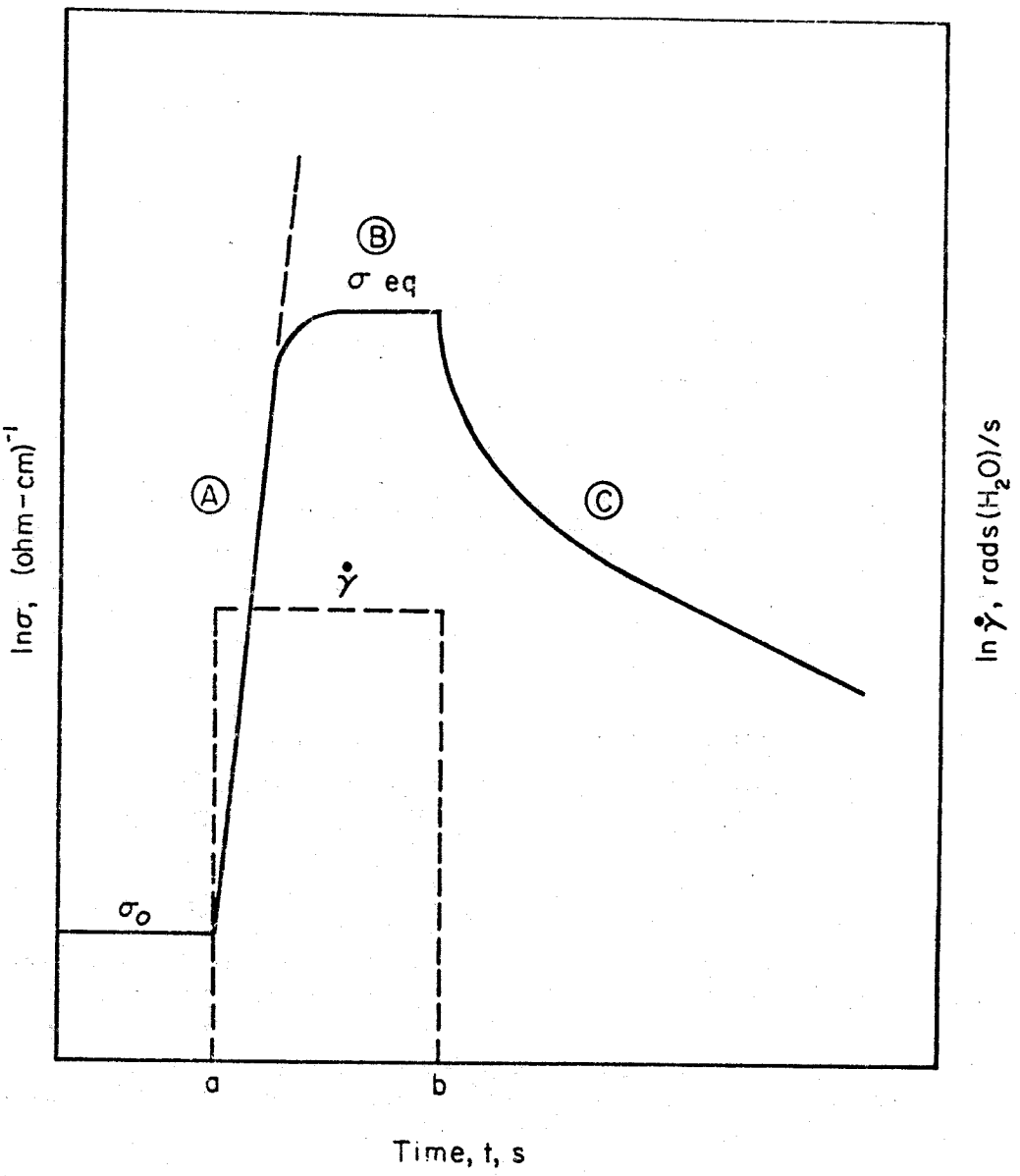

FIGURE 30 TYPICAL BEHAVIOR OF CONDUCTIVITY IN RESPONSE TO A RECTANGULAR PULSE OF GAMMA-RAY DOSE RATE[1]

Reference 17

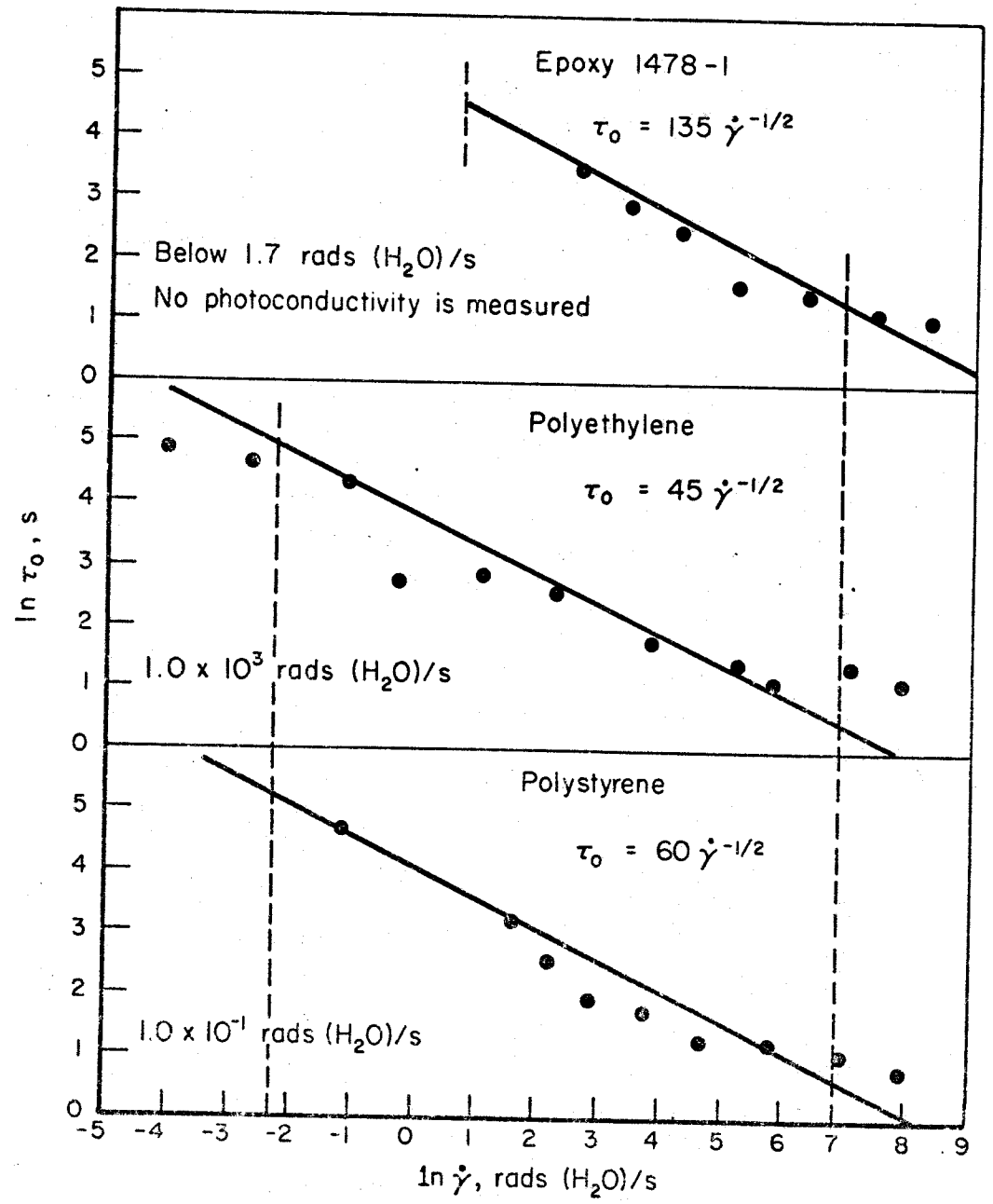

FIGURE 31 LOGARITHM OF TIME CONSTANT VERSUS LOGARITHM OF GAMMA-RAY DOSE RATE FOR POLYETHYLENE, POLYSTYRENE, AND EPOXY 1478-1 AT 38 C[1]

Reference 17

Figure 32 Reference 17

MEASUED VALUES OF A_γ AND δ FOR EIGHT MATERIALS AS DEFINED BY $(\sigma-\sigma_o) = A_\gamma \dot{\gamma}\ \sigma^{(a)}$

Material[b]	Temperature[c], C	δ	A_γ	Range of $\dot{\gamma}$, rads (H_2O)/s
Polystyrene	38	0.97	4.0×10^{-17}	1.7×10^{-2} to 5.0×10^{3}
	49	0.97	4.0×10^{-17}	1.7×10^{-2} to 5.0×10^{3}
	60	0.97	4.0×10^{-17}	1.7×10^{-2} to 5.0×10^{3}
Polyethylene	38	0.74	5.2×10^{-16}	8.3×10^{-2} to 1.7×10^{3}
	49	0.74	6.3×10^{-16}	8.3×10^{-2} to 1.7×10^{3}
	60	0.74	1.6×10^{-15}	8.3×10^{-2} to 1.7×10^{3}
Epoxy 1478-1	38	No measurable photoconductivity below $\dot{\gamma}$ = 1.7		
		1.0	3.3×10^{-17}	1.7 to 4.2×10^{3}
	49	No measurable photoconductivity below $\dot{\gamma}$ = 9.0		
		1.0	3.3×10^{-17}	9.0 to 4.2×10^{3}
	60	No measurable photoconductivity below $\dot{\gamma} = 7.5 \times 10^{1}$		
		1.0	3.8×10^{-17}	7.5×10^{1} to 4.2×10^{3}
Polypropylene	38	0.88	3.8×10^{-17}	1.8×10^{-3} to 6.0×10^{3}
H-film	38	1.1	5.8×10^{-18}	1.8×10^{-3} to 6.0×10^{3}
Teflon	38	1.0	1.2×10^{-16}	1.8×10^{-3} to 6.0×10^{3}
Nylon	38	No measurable photoconductivity below $\dot{\gamma}$ = 8.0		
		1.3	2.8×10^{-18}	8.0 to 6.0×10^{3}
Diallylphthalate	38	0.30	2.1×10^{-16}	1.8×10^{-3} to 3.0×10^{2}
		1.7	8.0×10^{-20}	3.0×10^{2} to 6.0×10^{3}

(a) Data taken under steady state conditions after 1.8×10^{3} seconds of electrification.

(b) Temperature is ± 1C.

(c) Fifteen samples of polyethylene, polystyrene, and Epoxy 1478-1 and three samples of the other materials were measured.

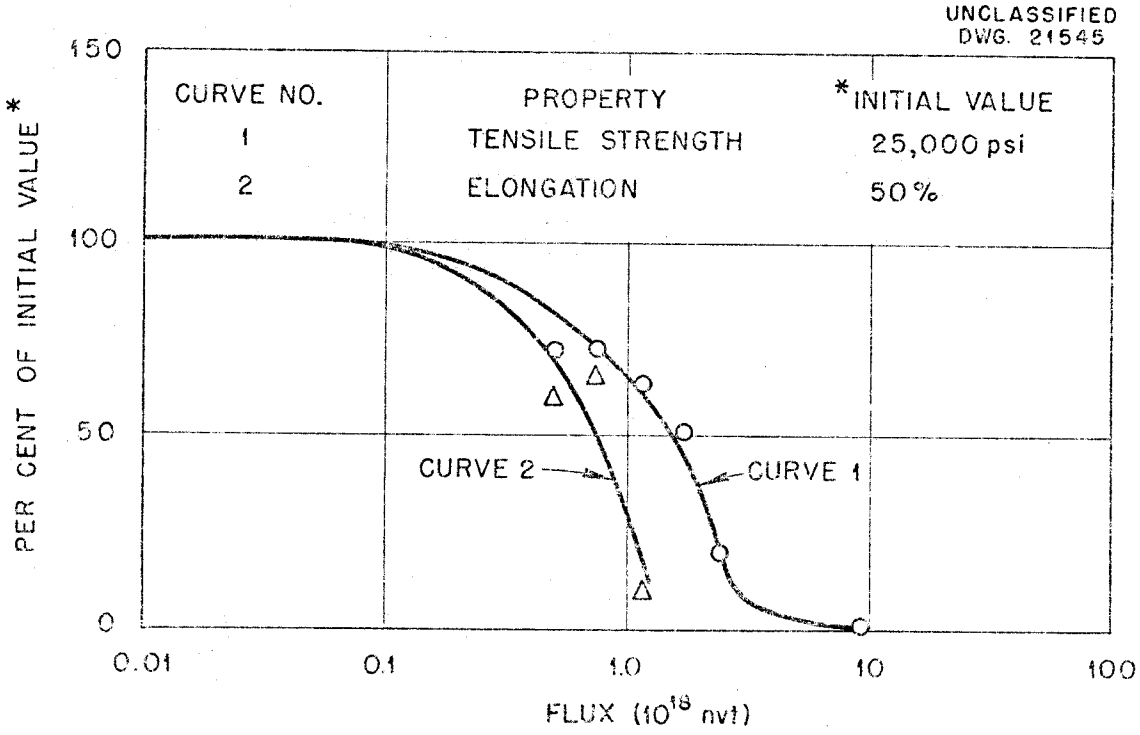

Figure 33 Physical Properties of Irradiated Mylar Film.

(Reference 20)

Flux to dose conversion

1 Megarad $\cong$ 2×10^{15} nvt

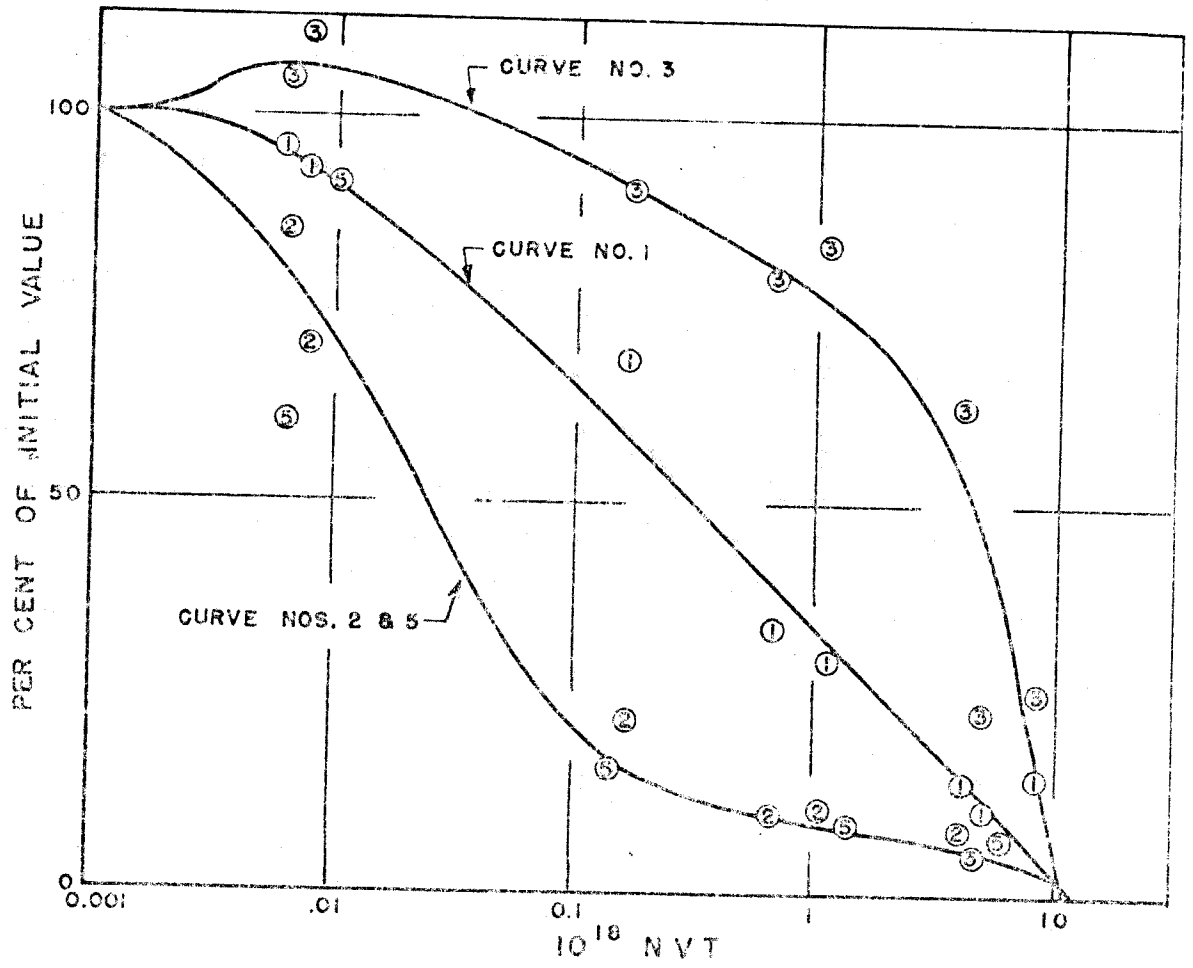

CURVE NO.	PROPERTY	INITIAL VALUE
1	TENSILE STRENGTH	11,000 LBS./SQ. IN.
2	ELONGATION	4.0 %
3	ELASTIC MODULUS	11 X 10^5 LBS./SQ. IN.
5	IMPACT STRENGTH	2.75 FT. LBS./IN. OF NOTCH

Figure 34 Mechanical Properties of Phenolic Linen Fabric Laminate (Reference 21)

Flux to Dose conversion

1 Megarads $\cong 3 \times 10^{15}$ nvt

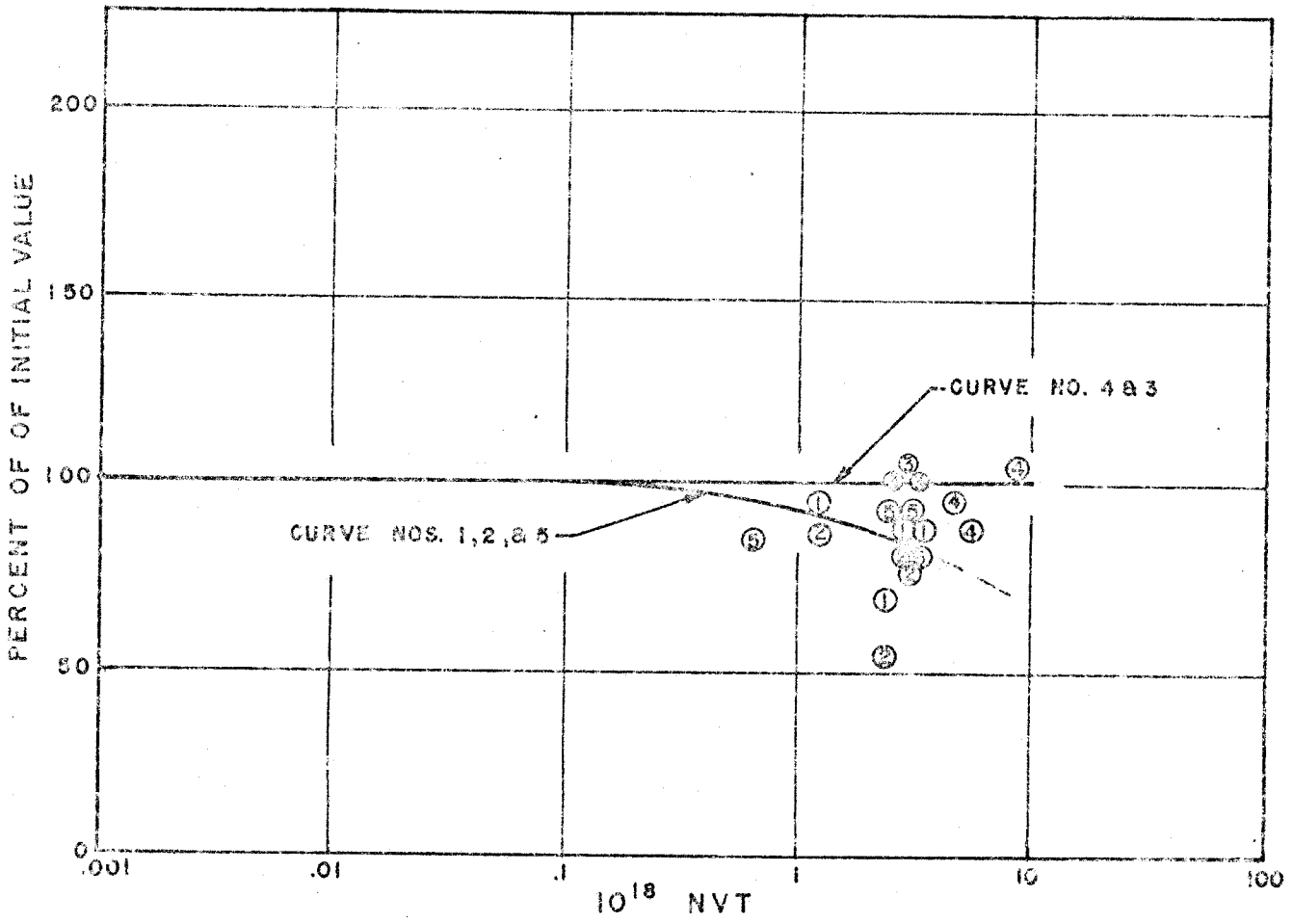

CURVE NO.	PROPERTY	INITIAL VALUE
1	TENSILE STRENGTH	12,200 LBS./SQ.IN.
2	ELONGATION	0.81 %
3	ELASTIC MODULUS	25×10^6 LBS./SQ. IN.
4	SHEAR STRENGTH	11,000 LBS./SQ. IN.
5	IMPACT STRENGTH	1.02 FT. LBS./IN. OF NOTCH

Figure 35 Fiber asbestos Phenolic (Reference 20)

Flux to Dose Conversion

1 Megarad = 5.5×10^{15} nvt

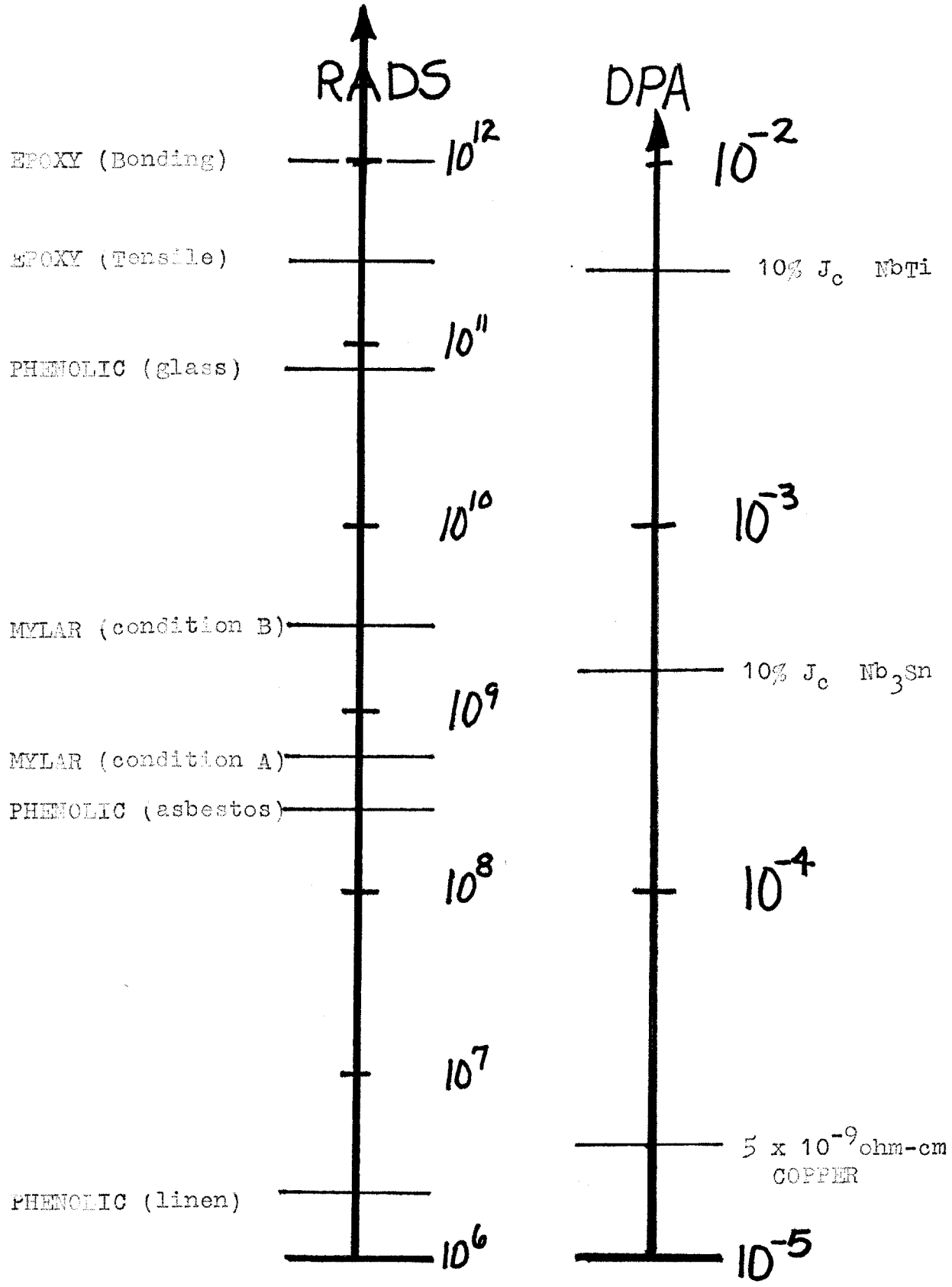

Figure 36 Radiation Dose Limits for UWCTR magnet system. No correlation has been made between rads and dpa and the relative position of these scales has been arbitrary.